

Calculations and Measurements of Raman Gain Coefficients of Different Fiber Types

Yuhong Kang

Thesis submitted to The Faculty of the Virginia Polytechnic Institute and State University
in partially fulfillment of the requirements for the degree of

Master of Science

In

Electrical Engineering

Roger H. Stolen, Chair,

Ira Jacobs

Ahmad Safaai-Jazi

December 9, 2002

Blacksburg, Virginia

Keywords: Fiber Raman amplifier, stimulated Raman scattering, effective Raman gain
and Raman gain coefficient, GeO₂ concentration, Effective area

Calculations and Measurements of Raman Gain Coefficients of Different Fiber Types

Yuhong Kang

Abstract

Fiber Raman amplification using the transmission line is a promising technology to increase the repeater distance as well as the capacity of the communication systems. Because of the growing importance of fiber Raman amplification, it is desired to predict the magnitude and shape of the Raman gain spectrum from the doping level and refractive index profiles of different fiber designs.

This thesis develops a method to predict the Raman gain coefficients and spectra for a pure silica core fiber and two different types of GeO₂-doped silica fibers given their index profiles. An essential feature of the model is the inclusion of the variation in Raman gain coefficient over the mode field due to the variation in the Ge concentration across the fiber core. The calculated Raman gain coefficients were compared with measurements of the peak Raman gain on a step-index GeO₂-doped fiber and with published measurements from various sources. Agreement between the calculated and measured peak gain for the step-index fiber was excellent. There was qualitative agreement with published measurements but there were significant differences between the calculated and published gain coefficients, which are not understood.

Part of the work sought a way of predicting Raman gain coefficients from a standard gain curve given only the fiber type and the effective area. This approach appears promising for moderately-doped fibers with the proper choice of effective area.

Acknowledgements

I would like to thank all of my committee members for their support and encouragement before and during my time spent at the fiber optics research group. I would like to acknowledge my advisor Dr. Roger Stolen for giving me the opportunity to work with him, for the help and advice, and for the valuable guidance and support of him during my graduate program.

I have enjoyed working with all the students in our group over the past 1 year. Special thanks to Nitin Goel for his so many advices on my thesis research.

I would also like to thank the continuous support and encouragement provided by my dear husband and parents.

Table of Contents

Abstract	ii
Acknowledgements.....	iii
Table of Contents.....	iv
List of illustrations.....	v
Chapter 1 - Introduction.....	1
1.1 Significance of Calculation and Measurement of Fiber Raman Amplifier	1
1.2 Overview of Raman Scattering	3
1.2.1 Spontaneous Raman Scattering	3
1.2.2 Raman Amplification using Stimulated Raman Scattering	6
1.3 Thesis Objective and Overview	8
Chapter 2 - Calculations of Raman Gain and Raman Gain Coefficients in Different Fiber Types	10
2.1 Theoretical Background	10
2.2 Calculations	16
2.2.1 Calculation parameters	16
2.2.1.1 Pure Silica Raman Gain Spectrum	16
2.2.1.2 Fiber Types	17
2.2.2 GeO ₂ concentrations and the refractive index.....	19
2.2.3 Simulation Results	23
2.2.3.1 Raman Gain Spectra for pure silica core fiber, step index fiber and dispersion-shift fiber	23
2.2.3.2 Optimized Effective Area Approximation Scheme.....	27
2.2.3.3 A simplified calculation model for standard step index fibers	32
Chapter 3 - Measurement of Raman Gain in Optical Fibers	40
3.1 Experimental Setup of Fiber Raman Gain Measurement	40
3.2 Experimental Results	42
Chapter 4 – Conclusions	46
4.1 Conclusions.....	46
4.2 Future Work.....	47
References.....	48
Vita	51

Table of Illustrations

Table 1.1 Comparison of commercial EDFA and FRA, data sheets from Amonics [9] ..	2
Figure 1.1 Spontaneous Raman Scattering	4
Figure 1.2(a) Parallel and Perpendicular Raman Gain Coefficients of [23].....	5
Figure 1.2(b) Parallel and Perpendicular Raman Gain Coefficients of Fused GeO ₂ [22]	5
Figure 1.3 The Relative Raman Cross Sections of Vitreous SiO ₂ , GeO ₂ , P ₂ O ₅ and B ₂ O ₅ glasses. [12]	6
Figure 2.1 Linear regression factor vs frequency shift (cm ⁻¹)[27].....	13
Figure 2.2 Parallel and Perpendicular Raman Gain Spectrum of fused Silica [23]	17
Table 2.1 Specifications for SMF-28 and SPECTRAN Fibers	18
Figure 2.3 Refractive index profile for SPECTRAN fiber	18
Figure 2.4 Refractive index profile for dispersion-shift fiber.....	19
Table 2.2 Sellmeier's Equation Parameters for Pure and GeO ₂ Doped Silica Glass	20
Figure 2.5 Refractive Index vs GeO ₂ concentration (Mol %).....	21
Figure 2.6 Index Difference vs GeO ₂ concentration (Mol %)	21
Figure 2.7 Refractive Index of Pure Silica and GeO ₂ -doped Silica vs Wavelength.....	22
Figure 2.8 Effective Raman Gain for dispersion-shift fiber, step index fiber, and pure silica core fiber	24
Figure 2.9 Normalized Raman Gain in Different Fibers	25
Table 2.3 Raman Gain Data in Different Fibers, In the Case of Depolarized Light	25
Figure 2.10 Raman Gain Coefficient with Different Fibers	26
Figure 2.11 Comparison of Raman Gains of All Fiber types with Four Effective Area Approximation Schemes.....	29
Figure 2.12 Comparison of Normalized Raman Gains of All Fiber Types with Four Effective Area Approximation Schemes	30
Figure 2.13 Comparison of Raman Gain Coefficients of All Fiber Types with Four Effective Area Approximation Schemes	31
Figure 2.14 Comparison of Raman gain curves with the simplified and original calculation model.....	34
Table 2.4 Measured Raman Gain For Different Transmission Fiber Types	38
Table 2.5 Comparisons between the Calculated and Published Measurement D For Different Transmission Fiber Types	38
Figure 3.1 Experimental setup for measuring Raman gain	41
Figure 3.2 Spectrum of the pump source	43
Figure 3.3 Pump on/off Optical Gain in dB	44

Chapter 1 - Introduction

1.1 Significance of Calculation and Measurement of Fiber Raman Amplifier

Distributed Fiber Raman Amplifier (FRA) using the transmission line as a Raman gain medium is a promising technology available for the long haul communication systems, especially for Wavelength Division Multiplexing (WDM), where simultaneous amplification of multi-channel lightwave signals is needed, as well as for repeaterless transmission, where optical gain is required for compensation of the fiber loss [1]-[5]. FRA is to amplify optical signals in optical fibers, based on transferring the power from the pump beam to the signal via Raman interaction between the light and vibrational modes of the glass. Typically, the Raman gain coefficient in fused silica peaks at a Stokes shift of about 13.2THz with a 3dB bandwidth of about 6THz. FRAs exhibit several attractive features for applications in transmission systems, which are listed as follows:

1. Simplicity of amplifier architecture: Raman gain is obtainable in any conventional transmission fiber. Only high pump lasers are required to be launched with the signals, and there is no excess loss in the absence of pump power.
2. Low noise: Distributed Raman amplifiers may deliver negative noise figures [6], while the Erbium Doped Fiber Amplifiers (EDFA) have at least 3dB noise figure, as shown in Table 1.1.
3. Broad gain spectrum: The Raman gain bandwidth is very broad, around 60nm in terms of Full Width at Half Maximum (FWHM), which is of significance to the wavelength division multiplexed system. One unique technique applicable for RFA is that a broader gain spectrum may be obtained by the use of multi-wavelength pump sources [7][8].
4. Flexibility of transmission window: The pump wavelength determines the gain spectrum of a Raman amplifier, which means the operation window is

adjustable. Furthermore, the multi-wavelength pump technique increases and flattens the bandwidth by pumping simultaneously at different wavelengths.

- Higher saturation power: Commercial Raman amplifiers have a saturation power over 100mW, compared to 50 mW with EDFA.

	PUMP POWER	BANDWIDTH	SATURATION POWER	NOISE
EDFA	35mW	37nm from 1528-1565 with flattening technology	50mW	5.5 dB
FRA	~350mW	100nm from 1520-1620 with 4 pumps		-2dB (C band) -3dB (L band)

Table 1.1 Comparison of commercial EDFA and FRA, data sheets from Amonics [9]

The spontaneous and stimulated Raman scatterings in silica-based glasses and optical fibers have been studied extensively, since the early work by Stolen [10], Lin [11] and Galeener [12]. The potential applications of Raman amplification in fibers for communications were first pointed out by Ippen, Patel and Stolen [13], because of the long interaction length and high light intensity associated with small core size of fibers. An early application of fiber Raman amplifier was as a discrete preamplifier to improve the receiver sensitivity [14]. It also can be used to post-amplify the signal before the signal is launched into the transmission lines. In 1992, 23 dB signal gain was obtained from a 140 ns pump pulse with 1.4 W peak power over 20-km-long dispersion shifted fiber [15]. In 1996, 30 dB gain was obtained when a heavily germanium-doped optical fiber was pumped with only 350mW [16]. Distributed Raman amplification used in conjunction with discrete in-line EDFAs can reduce the overall span noise figure more than 7dB assuming an EDFA noise figure of 4dB [17]. Recently, progress in high power diode lasers has offered great potential for the development of a multi-wavelength pumped FRAs to achieve 1dB flatness and ultrawide bandwidth over 100nm [18].

The important parameters to describe the gain of the FRA are the Raman gain coefficient and Raman gain coefficient over effective area, also called effective Raman gain, which is the desired parameter in a Raman amplifier. Knowing this number can give us a projection of how much signal gain can be achieved in a specific fiber given its length and attenuation parameters at pump and signal wavelengths. Recently the measurements of effective Raman gain of transmission fibers have been performed by several scientists to investigate the application of distributed Raman amplification [19]-[21]. However, their results are only qualitatively in agreement with each other. One of the reasons is that the fibers under test were from various types, different companies, and even for the same fiber type, the variations appear to be large. Consequently, to fully understand the material and fiber structure dependences of SRS and develop the multi-wavelength pumped Raman amplifiers, it is vital to design a reliable numerical simulation model associated with accurate measurements on Raman gain coefficients to predict obtainable Raman gains in optical fibers from the fiber designs. It is also important to find a simplified but sufficiently accurate model to evaluate the Raman gain spectrum of different fibers from their refractive index profiles.

1.2 Overview of Raman Scattering

Fundamentally, Raman Scattering can be divided into two categories: Spontaneous Raman Scattering and Stimulated Raman Scattering. To have a complete understanding of the Raman scattering, this section briefly reviews the history and principle of the Raman Scattering.

1.2.1 Spontaneous Raman Scattering

When an incident light of frequency ν_0 is scattering from molecules of a substance, the scattered light will consist mostly of light with the same frequency as the incident light. In the meantime, low intensities of light with frequency higher and lower than the incident light may also be observed. This is called spontaneous Raman scattering, which was observed independently and simultaneously by Landsberg, Mandelstam and Raman in 1928.

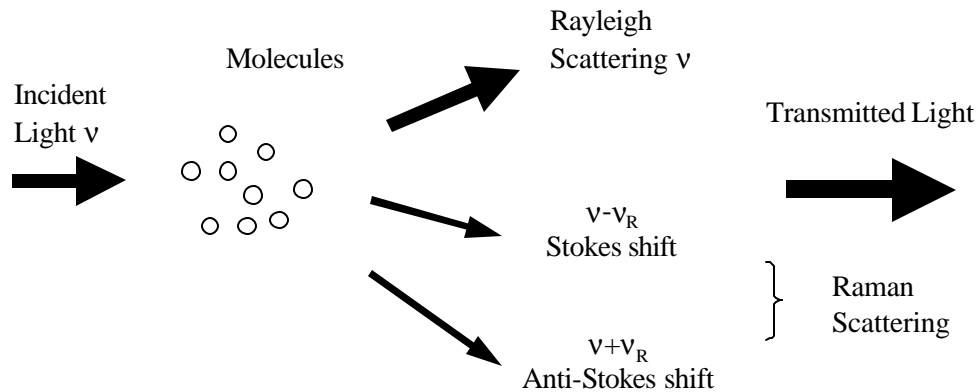


Figure 1.1 Spontaneous Raman Scattering

As shown in Figure 1.1, when a photon is incident with frequency ν_0 upon a molecule in some arbitrary vibrational state, it will excite the molecule to some intermediate state; and the molecule will immediately relax its energy state by emitting a photon. The molecule may return to a higher vibrational energy state than before. The resulting scattered light will be of a lower energy than the incident light ($h\nu_s < h\nu_i$); This is called Stokes scattering. The scattered light will have a higher energy ($h\nu_s > h\nu_i$) to form an anti-Stokes side band if the molecule was already in an excited vibrational state. Spontaneous Raman Scattering is a very useful analytical tool for the study of vibrational modes of solids, liquids and gases.

Due to the amorphous nature, fused silica and GeO_2 exhibit broad gain spectra over 20THz. The Raman gain spectra in fused silica and GeO_2 are shown in Figure 1.2 (a) and 1.2 (b), where the gain spectra are a composite of measurements by several authors of spontaneous Raman scattering in bulk silica, GeO_2 samples and silica-core fibers [22][23]. The two curves in each figure are for scattering of light polarized parallel and perpendicular to the polarization of the exciting light. The perpendicular gain coefficients in silica and GeO_2 are much less than the parallel ones.

The material related frequency shift dependent stimulated Raman scattering coefficient, g_R is related to the Zero Kelvin spontaneous Raman scattering cross section which will be discussed in detail in Chapter 2.

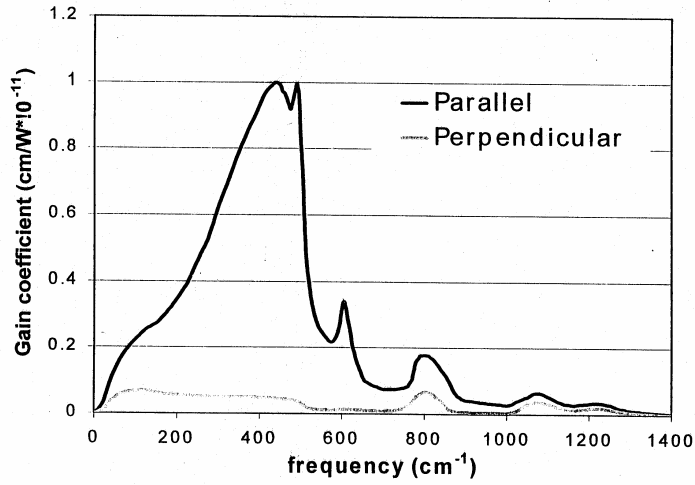


Figure 1.2(a) Parallel and Perpendicular Raman Gain Coefficients of [23]

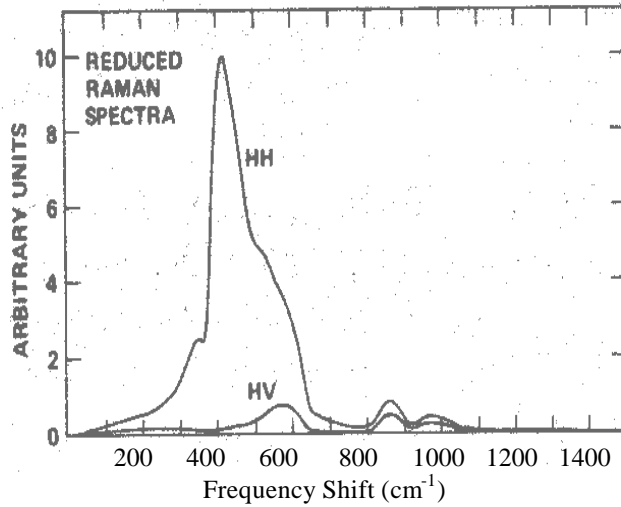


Figure 1.2(b) Parallel and Perpendicular Raman Gain Coefficients of Fused GeO_2 [22]

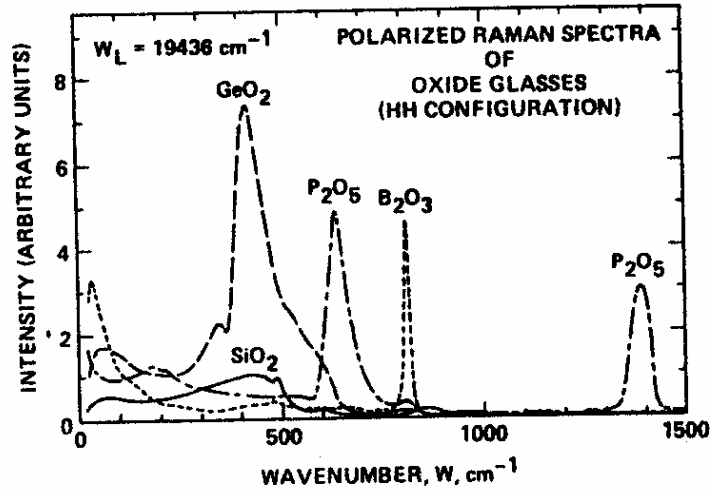


Figure 1.3 The Relative Raman Cross Sections of Vitreous SiO_2 , GeO_2 , P_2O_5 and B_2O_5 glasses. [12]

Figure 1.3 shows relative Raman cross sections of vitreous SiO_2 , GeO_2 , P_2O_5 and B_2O_5 glasses, normalized to the peak of the silica spectrum. These Oxide glasses are commonly used as dopants for fiber fabrication. After corrected for effects caused by different optical index of these glasses, the Raman cross section for pure GeO_2 at the peak is approximately nine times as high as that for pure SiO_2 . Doping GeO_2 into SiO_2 glass has been proved to significantly increase the Raman cross-section and the Raman gain coefficient for silica-based fibers.

1.2.2 Raman Amplification using Stimulated Raman Scattering

Optical amplification via stimulated Raman scattering, called Raman amplification, has advantages of self-phase matching between the pump and the signal, and broad bandwidth or high speed response, compared with other nonlinear processes.

When a weak signal is launched with a stronger pump, it will be amplified due to SRS. In the CW case, the signal amplification is described by the following equations in terms of power transfer from the pump to the signal due to the Raman interaction between the pump and the signal:

$$\frac{dP_S}{dz} = g_R P_P P_S - \mathbf{a}_S P_S \quad (1.1)$$

$$\frac{dP_P}{dz} = -\frac{\mathbf{w}_P}{\mathbf{w}_S} g_R P_P P_S - \mathbf{a}_P P_P \quad (1.2)$$

The Raman interaction transfers power from P_P to P_S . P_P and P_S are the powers of waves at frequencies \mathbf{w}_P and \mathbf{w}_S . P_P and P_S are functions of propagation distance Z and \mathbf{a}_P , \mathbf{a}_S stand for the fiber loss at \mathbf{w}_P and \mathbf{w}_S . g_R represents the Raman gain coefficient in a fiber. If we neglect the pump depletion term on the first right side of equation (1.2), we can obtain:

$$P_S(L) = P_S(0) \exp\left(g_R \frac{P_0}{A_{eff}} L_{eff} - \mathbf{a}_S L\right) \quad (1.3)$$

$$L_{eff} = \frac{1 - \exp(-\mathbf{a}_P L)}{\mathbf{a}_P} \quad (1.4)$$

The solutions show, because of pump absorption, the effective length L_{eff} in place of the actual fiber length L . For short lengths, the effective length approximates L , and for long length, it reaches $1/\mathbf{a}_P$. Clearly, high Raman gain can be achieved with high pump power, long effective lengths, small effective area, high stimulated Raman scattering gain coefficients as well as low signal and pump attenuations.

$$G = 4.34 \left[g_R L_{eff} \frac{P_0}{KA_{eff}} - \mathbf{a}_S L \right] \quad (1.5)$$

Signal gain G in dB depends on the pump intensity, the effective Raman gain coefficient, the effective length and the polarization state [23][24]. Since the polarizations of the pump and signal in conventional transmission fibers vary arbitrarily along the fiber, the net gain is a mixture of the parallel and perpendicular gains. This is

described by a polarization factor K, which is 1 if the pump and signal waves are polarization matched, or 2 if depolarized.

Effective area for Raman gain is determined by mode size and the overlap between pump and Stokes modes, and defined as:

$$A_{eff} = 2\mathbf{p} \frac{\int \mathbf{y}_p^2 r dr \int \mathbf{y}_s^2 r dr}{\int \mathbf{y}_R^2 \mathbf{y}_S^2 r dr} \quad (1.6)$$

Where \mathbf{Y}_p , \mathbf{Y}_s represent the mode fields at the pump and Stokes wavelengths.

The effective stimulated Raman gain and gain coefficients in GeO₂-doped fibers can be measured based upon the equation (1.5), and independently calculated through the spontaneous Raman cross section measured from the GeO₂-doped silica based glass as discussed in the next chapter.

1.3 Thesis Objective and Overview

The goal of this thesis is to develop a calculation model for predicting the Raman gains and Raman gain coefficients obtainable in different GeO₂-doped silica fibers given their fiber profiles. The measurement of the peak Raman gain using pump on/off method is performed using a step index GeO₂-doped silica fiber to support this simulation model. Some major factors affecting the Raman gain in a fiber are discussed in this thesis to characterize the distributed fiber Raman amplification and help us come up with a simplified model to estimate the Raman gain.

Chapter 1 gives a general introduction to the principles of optical amplification using Stimulated Raman scattering and its potential applications in telecommunications, and discusses the calculation of Raman gain in fibers. Chapter 2 presents the calculation model to relating the spontaneous Raman cross-section to the effective Raman gains and gain coefficients of different GeO₂-doped fibers. The effect of the mode field

penetrating into the fiber cladding is included in the calculation model. Also a simplified but sufficiently accurate calculation model is developed. In the end, the characteristics of simulated Raman gain spectra of different fiber types are discussed and compared with published measurement data. Chapter 3 describes the experimental setup to measure the peak effective Raman gain of a step index fiber. Some considerations to achieve accurate results and comparisons of experimental results with simulation results are also covered in this chapter. Chapter 4 gives a summary of this thesis, and lists the suggestions for future work.

Chapter 2 - Calculations of Raman Gain and Raman Gain Coefficients in Different Fiber Types

In order to predict the behavior of Stimulated Raman scattering in transmission fibers, which can be used for distributed amplification in optical fiber links, it is important to theoretically calculate the Raman gain spectra of the transmission fibers based on their refractive index profiles as well as attenuation spectra. In this chapter, the Raman gain spectra, ranging from 30 cm^{-1} (0.9 THz) to 700 cm^{-1} (21.0 THz) frequency shifts, for pure silica core fiber (Z-Fiber), Standard single mode fiber (SMF-28 and SPECTRAN) and dispersion-shifted fiber (DSF) are calculated. This calculation includes the field averaging effect over the doping profile. In fiber designs, effective area (A_{eff}) plays a crucial role in controlling the Raman gain in fibers, so the effect of a change in A_{eff} with wavelength, on Raman gain is also estimated and discussed. The calculated results for typical transmission fibers are found to be in qualitative agreement with published measurement results, but there are several discrepancies with the quantitative data.

2.1 Theoretical Background

A weak Stokes signal launched into a fiber with a stronger pump will be amplified due to SRS as discussed in the previous chapter. The amplification of the signal is described through the following equations [25].

$$P_s(L) = P_s(0) \exp\left(\frac{g_R(\nu) P_0 L_{\text{eff}}}{KA_{\text{eff}}} - \alpha_s L\right) \quad (2.1)$$

$$g_R(\nu) = \mathbf{s}_0(\nu) \cdot \frac{I_s^3}{c^2 h n(\nu)^2} \quad (2.2)$$

Where c is the velocity of light, h is Planck's constant, I_s is the Stokes wavelength, $n(\nu)$ is the refractive index, which is frequency dependent, and K is the polarization factor, which is 1 if the pump and signal waves are polarization matched, or 2 if depolarized. The spontaneous zero Kelvin Raman cross section $\mathbf{s}_0(\nu)$ is defined as the

ratio of radiated power at the Stokes wavelengths to the pump power at temperature 0K, which can be obtained with the measured Raman cross-section $\mathbf{s}_T(\nu)$ at temperature TK and the thermal population factor $N(\nu, T)$

$$\mathbf{s}_0(\nu) = \mathbf{s}_T(\nu) / (N(\Delta\nu, T) + 1) \quad (2.3a)$$

$$N(\Delta\nu, T) = \frac{1}{\exp\left(\frac{hc \Delta\nu}{K_B T} - 1\right)} \quad (2.3b)$$

The $g_R(\mathbf{n})$ in Equation 2.2 is the spontaneous Raman gain coefficient in bulk glass, where $g_R(\mathbf{n})$ is uniform in all directions. But for fibers, the Germania concentration, and hence the stimulated Raman gain coefficient, may vary across the whole fiber. As a result, $g_R(\mathbf{n})$ is also a function of the radial distance with respect to the core center. In addition, in a fiber the mode field penetrates into the cladding so that the effective Raman gain coefficient is some average over the doping profile. The proper way to include the increase in Raman gain from Ge-doping is to include Raman gain coefficients $g_R(\mathbf{n}, r)$ in the calculation of the overlap integral as shown in Equation 2.4.

Effective area is determined by mode size and the overlap between pump and Stokes modes as shown in Equation 1.6. Effective Raman Gain (g/A_{eff}) is defined as:

$$\frac{g_R}{A_{\text{eff}}} = \frac{\int g_R(\mathbf{n}, r) \mathbf{y}_p^2 \mathbf{y}_s^2 r dr}{2p \int \mathbf{y}_p^2 r dr \int \mathbf{y}_s^2 r dr} \quad (2.4)$$

Where $\mathbf{Y}_p, \mathbf{Y}_s$ represent the mode fields at the pump and Stokes wavelengths and g_R is the effective Raman gain coefficient of the fiber shown in Equation 2.1, which can be obtained by multiplying the effective Raman gain g_R/A_{eff} with A_{eff} . $g_R(\mathbf{n}, r)$ is the Raman gain coefficient in a fiber with a specific GeO_2 concentration at a certain radial distance to the core center, which is related to spontaneous zero Kelvin Raman cross-section $\mathbf{s}_0(\nu)$ through Equation 2.2.

Since the cross section $s_0(\nu)$ varies with n^4 , it is clearly seen from the equation (2.2) that Raman gain coefficient varies linearly with signal frequency.

The above equations are obtained under several assumptions. The first is that the bandwidth of the pump is much less than that of the Raman gain spectra. Secondly the equations assume that pump depletion due to the amplification of the signal is neglected in the case of a weak signal with a stronger pump.

Based on the research results of Galeener [12], Shibata [26] and Davey [27], the Raman cross section peak for pure GeO₂ is about 9 times as high as the pure SiO₂, and the Raman cross section of a GeO₂ doped silica glass is in linear relationship with Germanium concentration.

The change in Raman cross-section with GeO₂-doping mol% (x_{GeO_2}) in pure silica has been summarized in the expression:

$$s'_0(x_{GeO_2}, n) = s'_0(SiO_2, n) + C(n) \cdot x_{GeO_2} \quad (2.5)$$

Where $s'_0(SiO_2, n)$ and $s'_0(x_{GeO_2}, n)$ respectively represents the Raman cross-sections of pure silica and Ge-doped silica, normalized with respect to the peak Raman cross-section of pure silica and $C(n)$ is a linear regression factor whose values at different frequency shifts are obtained from the reference [27] and illustrated in Figure 2.1.

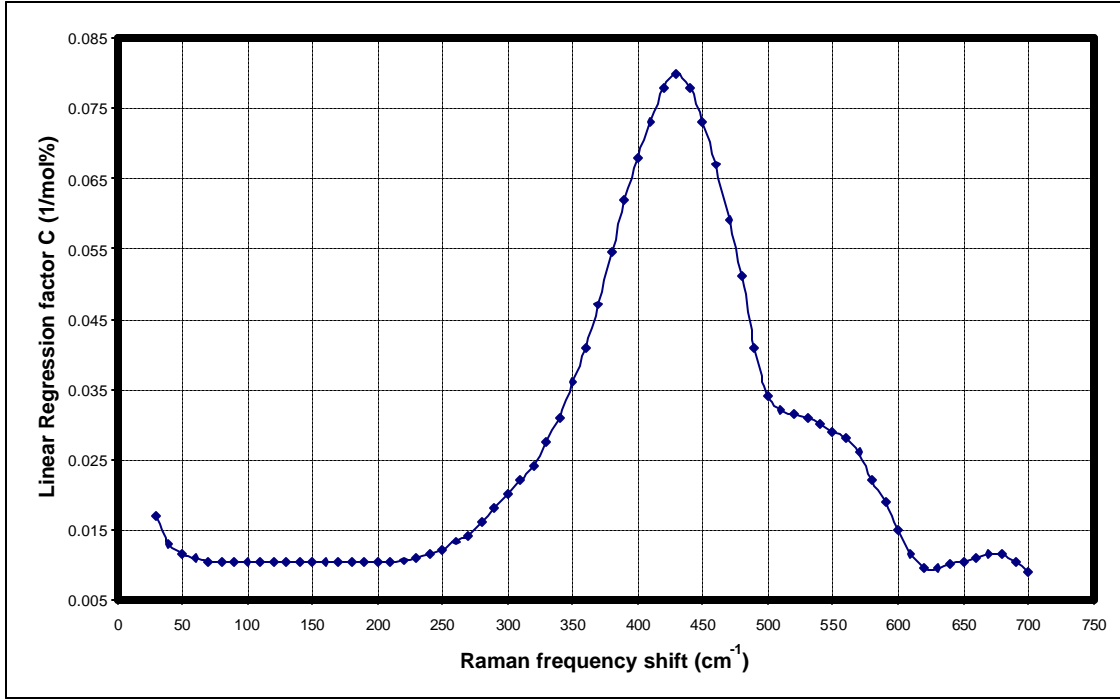


Figure 2.1 Linear regression factor vs frequency shift (cm^{-1})[27]

Now, if $\mathbf{s}_0(x_{\text{GeO}_2}, \mathbf{n})$ and $\mathbf{s}_0(\text{SiO}_2, \mathbf{n})$ represent non-normalized cross-sections and $\mathbf{s}_{0p}(\text{SiO}_2, \mathbf{n})$ represents the silica peak cross section, then equation (2.5) can be written as:

$$\frac{\mathbf{s}_0(x_{\text{GeO}_2}, \mathbf{n})}{\mathbf{s}_{0p}(\text{SiO}_2, \mathbf{n})} = \frac{\mathbf{s}_0(\text{SiO}_2, \mathbf{n})}{\mathbf{s}_{0p}(\text{SiO}_2, \mathbf{n})} + C(\mathbf{n}) \cdot x_{\text{GeO}_2}$$

or

$$\mathbf{s}_0(x_{\text{GeO}_2}, \mathbf{n}) = \mathbf{s}_0(\text{SiO}_2, \mathbf{n}) + C(\mathbf{n}) \cdot x_{\text{GeO}_2} \mathbf{s}_{0p}(\text{SiO}_2, \mathbf{n}) \quad (2.6)$$

Based on Equation 2.2, the Raman gain coefficients $g_R(\text{SiO}_2, \mathbf{n})$ and $g_R(x_{\text{GeO}_2}, \mathbf{n})$ for pure silica and for GeO_2 -doped silica respectively can be written as:

$$\begin{aligned}
g_R(x_{GeO_2}, \mathbf{n}) &= \mathbf{s}_0(x_{GeO_2}, \mathbf{n}) \cdot \frac{I_s^3}{c^2 h n_1^2} \\
g_R(SiO_2, \mathbf{n}) &= \mathbf{s}_0(SiO_2, \mathbf{n}) \cdot \frac{I_s^3}{c^2 h n_2^2}
\end{aligned} \tag{2.7}$$

where n_1 and n_2 are the refractive indices in a GeO_2 -doped silica core and a pure silica cladding of a fiber respectively. Even though refractive index is wavelength dependent, if the spectra being investigated are within a narrow range from 1457nm to 1614nm, n_1 and n_2 are treated as constant values using the refractive indexes at 1550nm. From equation (2.5) and (2.7) we get,

$$g_R(x_{GeO_2}, \mathbf{n}) = \frac{n_2^2}{n_1^2} \left[g_R(SiO_2, \mathbf{n}) + c(\mathbf{n}) \cdot x_{GeO_2} \cdot g_{Rp}(SiO_2, \mathbf{n}) \cdot \frac{I_s^3}{I_{sPeak}^3} \right] \tag{2.8}$$

Equation 2.8 applies to a fiber for which the pump and Stokes waves maintain the same state of polarization as they travel along the fiber. This is not true for transmission fibers when the states of polarization of pump and signal waves evolve randomly along the fibers and are seldom the same. It can be shown rigorously that if the perpendicular Raman gain is zero then the net Raman gain in a non-PM fiber is $\frac{1}{2}$ the parallel gain [28][29]. It is not clear whether this $\frac{1}{2}$ also applies to the perpendicular gain. But in the absence of full knowledge, a reasonable assumption for the net Raman gain coefficient in a non-PM fiber is to add half the parallel and half the perpendicular gain coefficients. The net depolarized peak gain at a Stokes wavelength of 1.0um in pure silica then becomes $1.046 \times 10^{-13} / 2 \text{ mW}^{-1}$, equal to $0.5023 \times 10^{-13} \text{ mW}^{-1}$. From figure 2.2, it can be clearly seen that the perpendicular gain coefficients has a large effect for frequency shift below 200 cm^{-1} , even though it is much smaller compared to the parallel one.

Very little is known about the perpendicular Raman gain coefficients of GeO_2 -doped silica. But ideally there would be a $C_{\perp}(\mathbf{n})$ for the perpendicular gain. As an approximation, following equation 2.6, the perpendicular gain of GeO_2 -doped silica would:

$$\mathbf{s}_{0\perp}(x_{GeO_2}, \mathbf{n}) = \mathbf{s}_{0\perp}(SiO_2, \mathbf{n}) + C_{\perp}(\mathbf{n}) \cdot x_{GeO_2} \mathbf{s}_{0p}(SiO_2, \mathbf{n}) \quad (2.9)$$

where $C_{\perp}(\mathbf{n})$ would be normalized to the peak $C_{\parallel}(\mathbf{n})$. Thus the total Raman gain coefficient of GeO₂ - doped silica for the average of random polarization states becomes:

$$g_{TOT}(x_{GeO_2}, \mathbf{n}) = \frac{n_2^2}{2n_1^2} [A + B] \quad (2.10)$$

$$A = g_{R\parallel}(SiO_2, \nu) + g_{R\perp}(SiO_2, \nu) \quad (2.11)$$

$$B = [C_{\parallel}(\nu) + C_{\perp}(\nu)] \cdot x_{GeO_2} \cdot g_{Rp\parallel}(SiO_2, \nu) \cdot \frac{I_s^3}{I_{sPeak}^3} \quad (2.12)$$

Figure 2.2 shows that the perpendicular gain curve of pure silica is much flatter than parallel one over the frequency shift ranging from 50-500cm⁻¹. By analogy with pure silica, $\mathbf{s}_{0\perp}(x_{GeO_2}, \mathbf{n})$ will probably be about 1/3 of $\mathbf{s}_{0\parallel}(x_{GeO_2}, \mathbf{n})$ at frequency shift 100 cm⁻¹. Thus, $C_{\perp}(\mathbf{n})$ can be approximated as a constant about 1/3 of $C_{\parallel}(\mathbf{n})$ at frequency shift of 100 cm⁻¹ over frequency shift ranging from 50-500cm⁻¹.

Also because the Raman gain coefficient varies linearly with signal frequency, the depolarized Raman gain coefficient obtained through Equation (2.10) at Stoke wavelength 1micron needs to be converted into the one at actual Stokes wavelengths I_s by dividing the Raman gain coefficient by the Stokes wavelength. So equation (2.10) can be modified to the following form

$$g_{TOT}(x_{GeO_2}, \mathbf{n}) = \frac{n_2^2}{2n_1^2} \left[\frac{A}{I_s} + \frac{B}{I_{sPeak}} \right] \quad (2.13)$$

where I_{sPeak} I_s values are in units of microns. Equation (2.13) gives us the Raman gain coefficient as a function of Stokes wavelength and GeO₂ concentration in GeO₂ doped silica.

As discussed before, because the Germanium concentration in a fiber may vary across the whole fiber, $g_{TOT}(x_{GeO_2}, \mathbf{n})$ is also a function of the radial distance with respect to the core center.

In our calculations equation (2.13) is used to find $g_{TOT}(x_{GeO_2}, \mathbf{n}, r)$, which is substituted into equation (2.4) to get the effective Raman gains for all fiber types. Raman gain coefficient in a fiber can be obtained by multiplying the effective Raman gain with the calculated effective area.

2.2 Calculations

To investigate the effects of Ge-doping and fiber structure on Raman gain and Raman gain coefficients of typical transmission fibers, the simulations of Raman gain and Raman gain coefficients are performed on a pure silica core fiber (PSCF), two standard step index fibers (SMF-28 and SPECTRAN) and a dispersion-shifted fiber (DSF). All these fibers except the pure silica core fiber are GeO₂-doped in the core with pure silica in the cladding.

2.2.1 Calculation parameters

In this simulation, pump wavelength is set at 1450.4nm for all fiber types. Referred to the frequency shift of 30-700cm⁻¹, the Stokes wavelength is from 1457nm to 1614nm, and the peak gain wavelength is 1549.27nm.

2.2.1.1 Pure Silica Raman Gain Spectrum

Raman gain spectrum for fused silica is shown in Figure 2.2 [23]. This figure forms the basis for estimation of Raman gain spectra in different fiber types as shown in equations (2.13) and (2.4). The red and yellow curves stand for scattering of light polarized parallel and perpendicular to the polarization of the exciting light. The blue curve is for the total (Parallel + Perpendicular) scattering of light. The absolute value of the total peak gain coefficient in this curve is 1.046×10^{-11} cm/W at a frequency shift of 440 cm^{-1} (13.2 THz), with 1.0 micron Stokes wavelength and second gain peak is at about 490 cm^{-1} (14.7 THz) frequency shift. Based on this figure, calculations of effective Raman gain and gain coefficients for pure silica core fiber, standard step index fiber and dispersion-shifted fiber are addressed in the following sections.

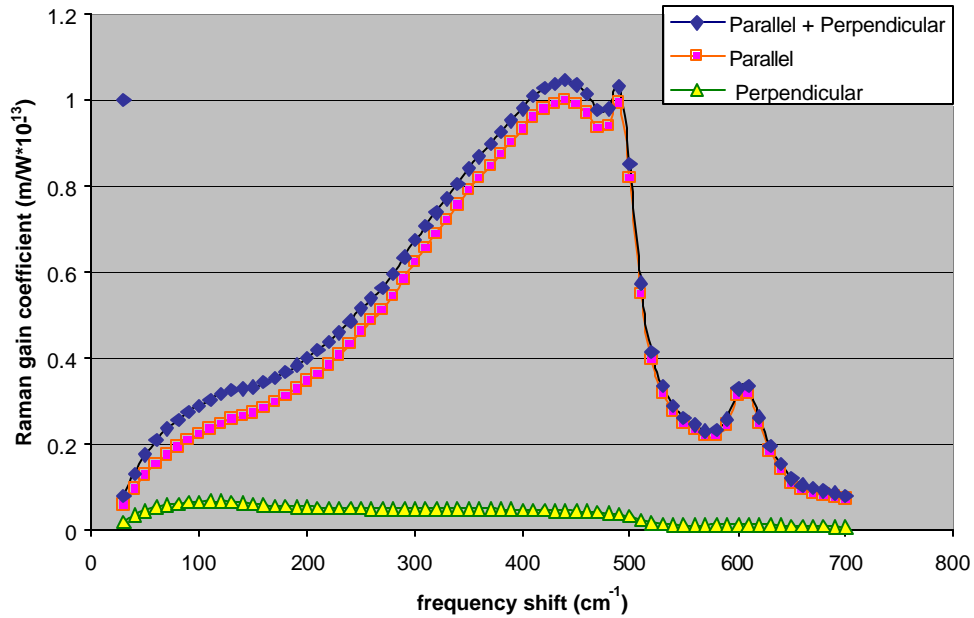


Figure 2.2 Parallel and Perpendicular Raman Gain Spectrum of fused Silica [23]

2.2.1.2 Fiber Types

The numerical simulations are performed on three typical transmission fibers: pure silica core fiber, standard step index fiber, and dispersion-shifted fiber.

1. Pure silica core fiber (PSCF), also called Z-fiber

For this Z fiber, the core and cladding diameter is respectively 9.7um and 125um. The index difference is 0.005 at 633nm wavelength. These numbers are based on measurements of 2 fibers taken at Bell laboratories in 1996 [30].

2. Standard step index fiber

Two types of standard step index fiber are used for the calculations. The first is SMF-28, manufactured by Corning cable. The second is a fiber sample donated by SPECTRAN Inc., which is also used for our measurements to check with the calculation results. The fiber parameters are listed as followed:

	Core Diameter (um)	Index Difference (632.8nm)	MFD @ 1310 nm (um)	Attenuation @ 1550 nm (dB/km)	Cutoff Wavelength (nm)
SMF-28	8.2	0.005265	10.4 ± 0.8	<0.25	<1260
SPECTRAN	8.3	0.00462	9.2	0.21	1258

Table 2.1 Specifications for SMF-28 and SPECTRAN Fibers

The fiber profile of the SPECTRAN fiber measured by YORK fiber profiler is shown in Figure 2.3.

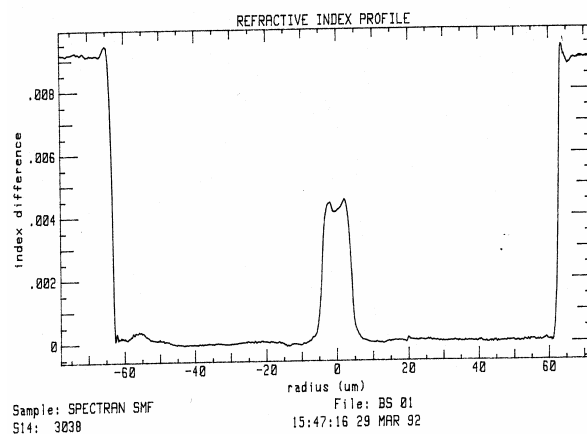


Figure 2.3 Refractive index profile for SPECTRAN fiber

3. Dispersion-shifted fiber (DSF)

The Refractive index profile of this fiber is shown in Figure 2.4. The fiber profile taken from the reference [31], is typical of many DSF fibers.

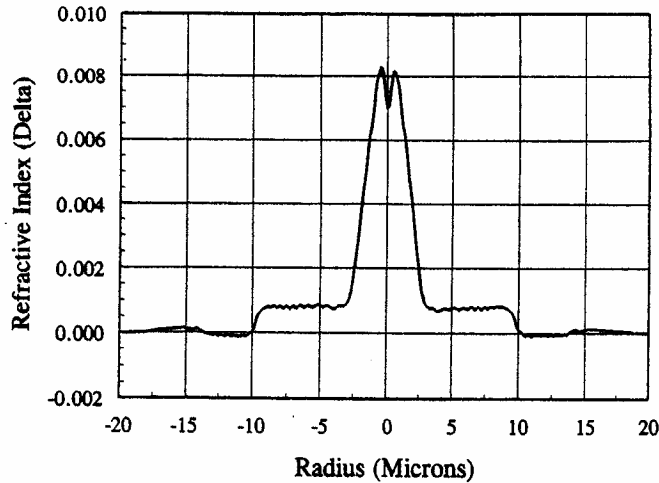


Figure 2.4 Refractive index profile for dispersion-shift fiber

2.2.2 GeO_2 concentrations and the refractive index

This section describes how to find the GeO_2 concentrations given a fiber profile and discusses the wavelength dependence of the refractive index.

The refractive-index relationship with the wavelength and the concentration is given by Sellmeier's equation:

$$n^2 = 1 + \sum_{i=1}^k \frac{a_i \times I^2}{I^2 - b_i} \quad (2.14)$$

where k is equal to 3, represents that this is a three term Sellmeier's equation. I is in a unit of micron. In this equation, a certain set of parameters a_i and b_i are corresponding to a specific type of material such as pure silica or GeO_2 -doped silica glass with a

certain GeO₂ concentration level. A series of a_i and b_i have been computed from the measured data taken from reference [32], as shown in Table 2.2.

Dopant (mol%)	a1	a2	a3	b1	b2	b3
Pure Silica	0.6965325	0.4083099	0.8968766	0.004368309	0.01394999	97.93399
GeO ₂ 6.3	0.7083925	0.4203993	0.8663412	0.007290464	0.01050294	97.93428
GeO ₂ 8.7	0.7133103	0.4250904	0.863198	0.006910297	0.01165674	97.93434
GeO ₂ 11.2	0.7186243	0.4301997	0.8543265	0.004026394	0.01632475	97.9344
GeO ₂ 15.0	0.7249180	0.4381220	0.8221368	0.007596374	0.01162396	97.93472
GeO ₂ 19.3	0.7347008	0.4461191	0.8081698	0.005847345	0.01552717	97.93484

Table 2.2 Sellmeier's Equation Parameters for Pure and GeO₂ Doped Silica Glass

By adopting Sellmeier equation with parameters given in the above table, we can get a figure of refractive index vs GeO₂ concentration (Mol %) at a certain wavelength. The calculated data of refractive index as a function of GeO₂ concentration at two wavelengths of 632.8nm and 1550nm are shown in Figure 2.5. It indicates a linear relationship between refractive index and GeO₂ concentration. The linear functions can be obtained by curve regression. Consequently, once the refractive index is known, the corresponding GeO₂ concentration can be found through the linear functions.

As shown in Figure 2.6, GeO₂ concentration also is found to increase linearly with the index difference from the pure silica if the refractive index line in Figure 2.5 at a certain wavelength is subtracted by the refractive index of pure silica at this wavelength.

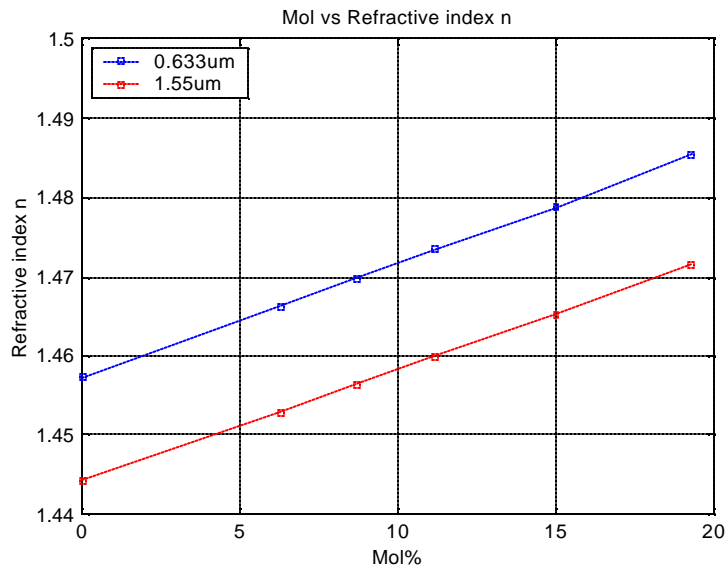


Figure 2.5 Refractive Index vs GeO₂ concentration (Mol %)

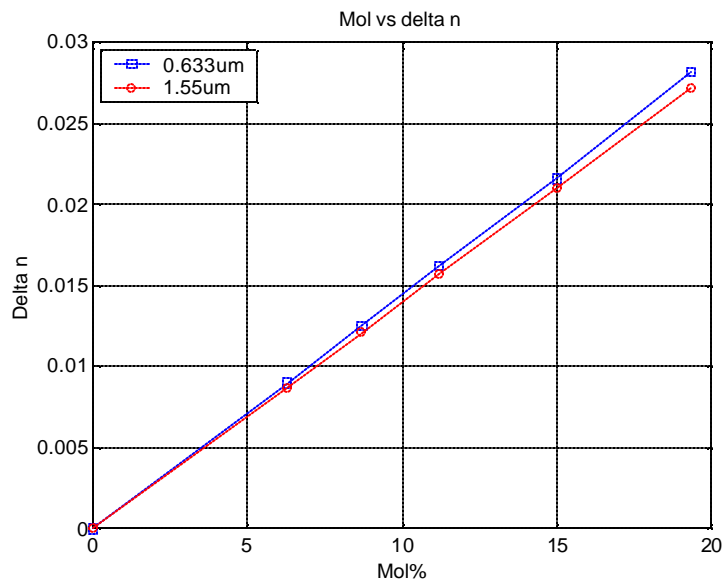


Figure 2.6 Index Difference vs GeO₂ concentration (Mol %)

As seen in Figure 2.6, the index differences between 632.8nm and 1550nm differ more with higher GeO₂ doping than with lower doping.

Through Sellmerier’s Equation, the wavelength dependence of the refractive index can be obtained as seen in Figure 2.7. The refractive index decreases linearly with the wavelength from 1457 nm to 1614 nm, while it increases with GeO₂ concentration. In addition, within a small wavelength range as from 1457nm to 1614nm, the variations in refractive index are shown in Figure 2.7, to be less than 0.2%. This variation is so small that the refractive indices of the core and the cladding can both be treated as constant values at 1550nm throughout this simulation for the step index fibers.

It is concluded that the GeO₂ concentrations across a fiber can be obtained if the fiber profile is provided.

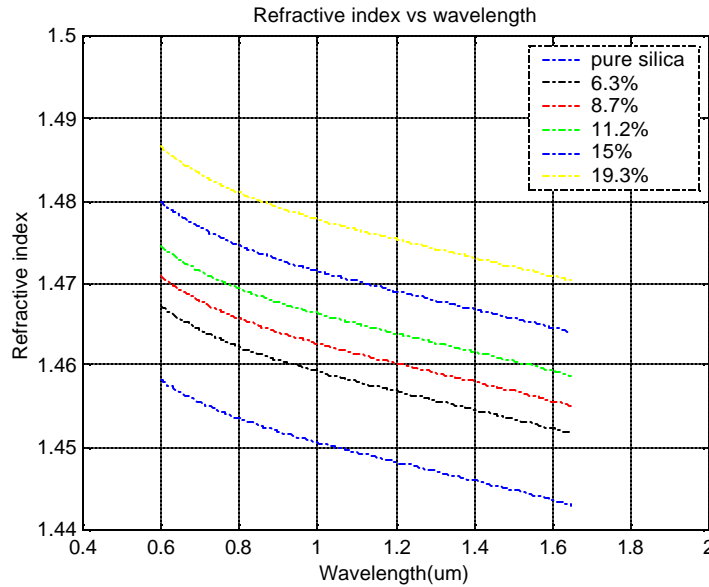


Figure 2.7 Refractive Index of Pure Silica and GeO₂-doped Silica vs Wavelength

2.2.3 Simulation Results

In this section, the calculated effective Raman gain and gain coefficients of different fibers are presented and compared with published data. Also a simplified model to predict the effective Raman gain is developed and discussed. It is noted that only LP01 mode exists in all four types of fibers investigated since the transmission window is set around 1550 nm, far beyond their cutoff wavelengths. The LP01 modes at pump wavelength 1450.4nm and signal wavelengths ranging from 1457 nm to 1614 nm are calculated using a commercial fiber program package with input of a fiber profile measured at 632.8nm; Thereafter, the effective areas and effective Raman gain spectra over the above wavelength range can be obtained through these LP01 modes.

2.2.3.1 Raman Gain Spectra for pure silica core fiber, step index fiber and dispersion-shift fiber

Figure 2.8 shows a plot of calculated effective Raman gains vs frequency shift for all the fiber types we investigated. The effective areas and effective Raman gains are calculated based on the equations (1.6), (2.4) and (2.13), where $g_R(x_{GeO_2}, \mathbf{n})$ is included in the overlap integral of the modes fields at the pump and the actual Stokes wavelengths.

According to the fiber parameters shown in the Table 2.1, Figure 2.3 and Figure 2.4, through Sellmeier equation (2.10), the dispersion-shifted fiber has the highest GeO₂ concentration, around 8.3 mol% near the core center, the SMF and SPECTRAN have respectively 3.71 mol% and 3.265 mol% GeO₂ in the core, while Z fiber has no GeO₂ in the fiber. Since there is no GeO₂ doping in the core and cladding of Z fiber, there is no change in the Raman gain coefficient of Z fiber, but the mode fields do affect the resultant Raman gain through the effective area A_{eff} . A comparison of the effective areas, GeO₂ concentration and peak Raman gain values for all these fibers can be found in Table 2.3. The effective areas listed in this table are calculated at pump wavelength

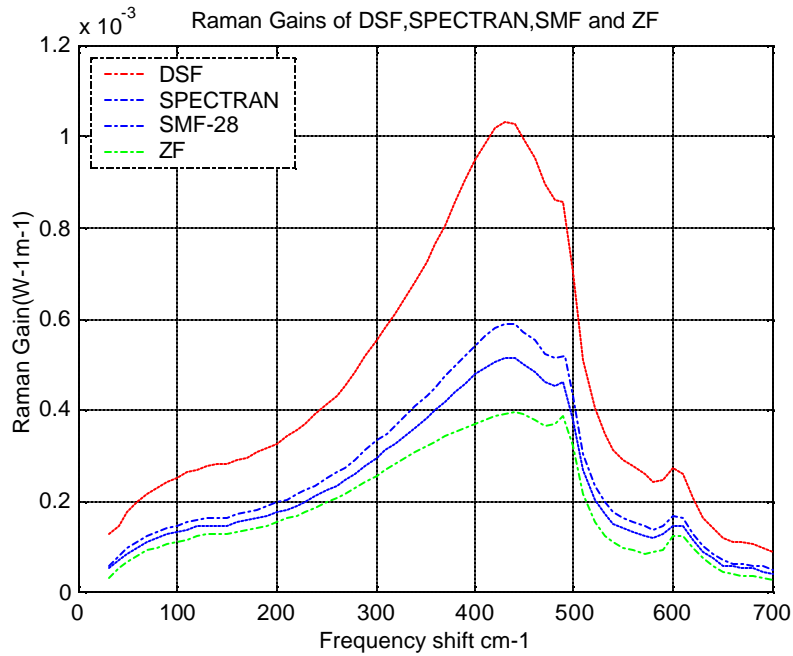


Figure 2.8 Effective Raman Gain for dispersion-shift fiber, step index fiber, and pure silica core fiber

of 1450nm and peak gain wavelength of 1550nm. It is clearly visible from Figure 2.8 and Table 2.3 that Raman gain increases with GeO_2 concentration and decreases with effective area, which depends on the fiber structure as well as GeO_2 concentration. The increase of Raman gain is the biggest in the case of DSF because of the highest GeO_2 -doping and the smallest effective area, on the other hand, the Z fiber has the least gain at 440cm^{-1} and the largest effective area. For example, at the frequency shift of 440cm^{-1} , DSF has a peak gain of $10.3 \times 10^{-4} \text{W}^{-1}\text{m}^{-1}$, which is 75% higher than that of the SMF-28; Peak gain and GeO_2 concentration of SPECTRAN fiber are both 12% less than that of those of the SMF-28.

Raman gain spectra were normalized to 1.0 at the peak gain to compare the overall gain profiles. As shown in Figure 2.9, Full Bandwidth Half Maximum (FWHM) decreases slightly with GeO_2 doping. But The FWHM of the two standard step index fibers (STF) SMF and SPECTRAN are almost same and both Raman gain curves are observed to be very close to each other. It implies that GeO_2 concentration in standard step index fibers

does not affect the gain profile very much even though it does change the effective Raman gain. FWHM values for all fiber types are also shown in Table 2.3. The second peak at around 490 cm^{-1} (14.7 THz) for Z fiber is observed to be the highest, while the DSF has the least. We can conclude from Table 2.3 and Figure 2.9 that the second peak suppresses as the GeO_2 concentration increases. In the meantime, the peak of the Raman gain curve moves to lower frequency shift associated with higher GeO_2 doping.

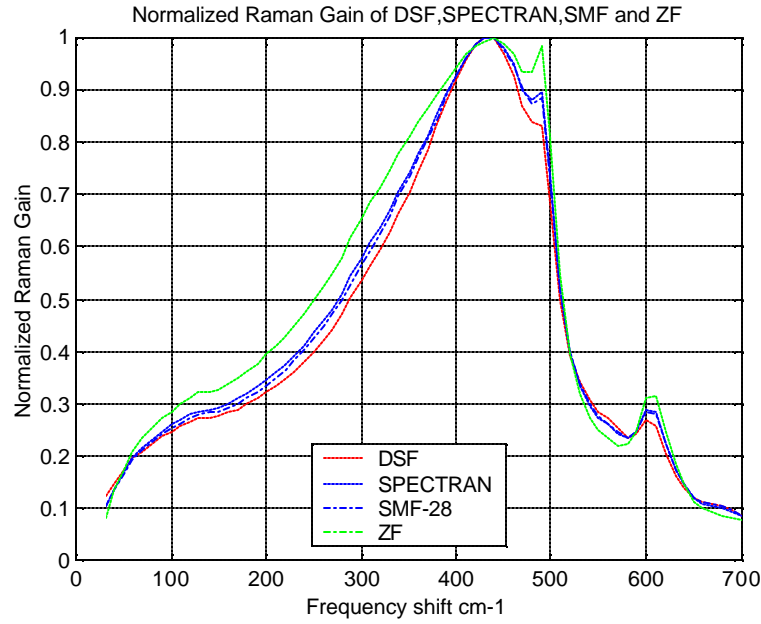


Figure 2.9 Normalized Raman Gain in Different Fibers

	DSF	SMF-28	SPECTRAN	ZF
A_{eff} at Peak Gain ($*1\text{E-}12\text{ m}^2$)	46.7	72.8	80.4	85.5
GeO_2 concentration (mol%)	8.3(peak)	3.71	3.265	0
Peak Gain (g/A_{eff}) ($*1\text{E-}4\text{ m}^{-1}\text{w}^{-1}$)	10.30	5.879	5.175	3.947
Peak Gain Coefficient ($*1\text{E-}13\text{ mw}^{-1}$)	4.811	4.279	4.172	3.374
Peak Gain frequency shift (cm^{-1})	430	440	440	440
Gain FWHM (nm at 1450nm pump)	52	55	56	62

Table 2.3 Raman Gain Data in Different Fibers, In the Case of Depolarized Light

The effective Raman gain coefficients shown in Figure 2.10, were calculated by multiplying the effective Raman gain with the effective areas. Figure 2.10 indicates that the peak gain coefficients of fibers also increase with GeO_2 doping, but not as significantly as the effective Raman gain. Pure silica core fiber has the same gain coefficient as the fused silica as expected.

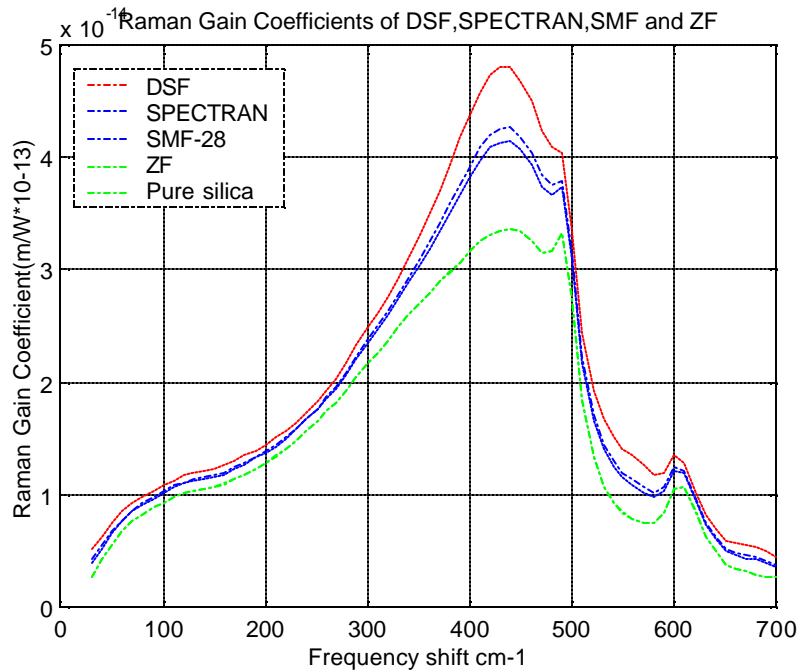


Figure 2.10 Raman Gain Coefficient with Different Fibers

2.2.3.2 Optimized Effective Area Approximation Scheme

As effective area depends on not only the mode field of the pump, but also those of the signals, A_{eff} is normally obtained using both Ψ_p and Ψ_s . However, based on the fact that Raman amplifiers are desired to operate around the peak zone, it is efficient not to find Ψ_s at each Stokes wavelength when calculating Raman gain spectra. To simplify the calculations, we need to find the optimized effective area approximation scheme by taking approximated signal wavelengths. The effective areas are obtained by taking the following four cases into considerations, from which we also can investigate how effective area affects the effective Raman gain and gain coefficient.

- 1) Both pump and signals wavelengths are taken to be 1450.4 nm.
- 2) Both pump and signals wavelengths are taken to be 1550 nm
- 3) Pump is 1450.4 nm and signal wavelengths are all set at 1550 nm.
- 4) Pump is 1450.4 nm and signal wavelengths are taken at actual Stokes wavelengths ranging from 1457 to 1614nm.

Figure 2.11 shows the simulation results of the effective Raman gains of all the fibers for the above listed 4 cases. Among these four cases, the first three are used to evaluate approximations and the last one is to get the actual values. For all fibers, the first case gives the highest effective Raman gain, g_R/A_{eff} , while the second case gives the least. These results are theoretically justified because the smaller effective area, the bigger Raman gain, and the effective area at 1450nm is smaller than that at 1550nm.

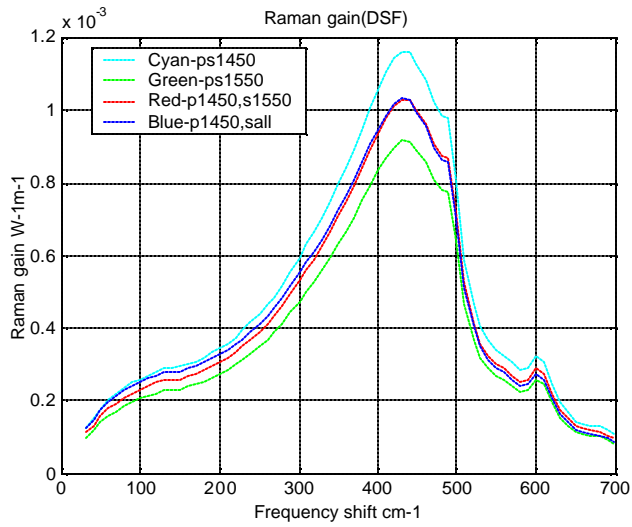
As to the third and the last case, these two Raman gain curves are very close to each other except the lower ends of the curves, which gives 5% difference of Raman gain. Both are kind of average of the first and the second cases. This comparison leads us to an optimized approximation that we can use the third case, in which pump is at 1450 nm and signal is at 1550 nm, to approximate the actual gain spectrum.

Figure 2.12 compares the normalized Raman gain curves with respect to the peaks for all four cases to find the change in the gain profiles due to this effective area scheme.

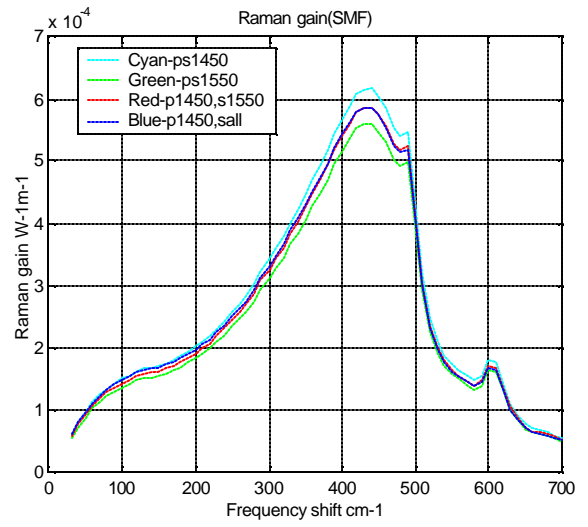
The comparison demonstrates that the normalized Raman gain curves are very close to each other in all cases and the effective area affect little on the shape of the Raman gain curve.

Figure 2.13 shows the Raman gain coefficient curves for the four cases are also very close to each other. It means the influence of the effective area on the Raman gain coefficient is neglectable.

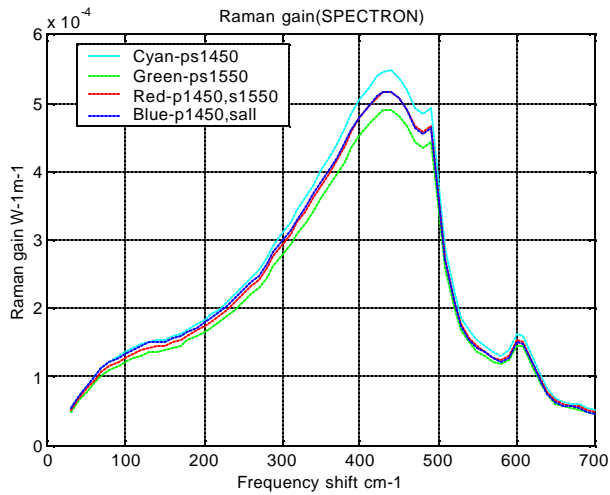
In conclusion, an optimized approximation can be achieved by using pump at 1450 nm and signal at 1550 nm to approximate the actual effective areas.



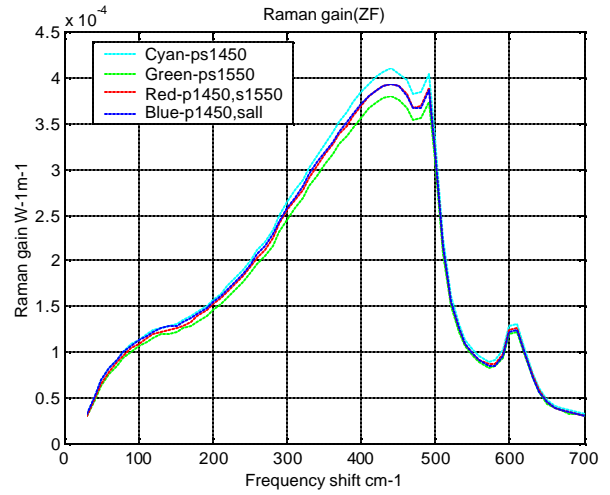
1) Dispersion Shift Fiber



2) SMF-28

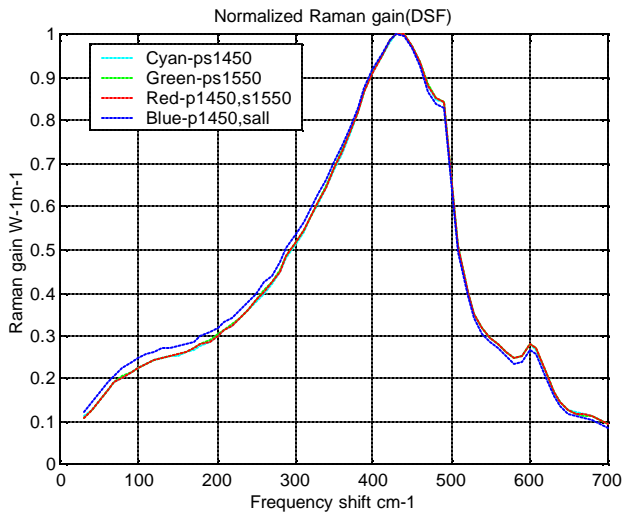


3) SPECTRAN

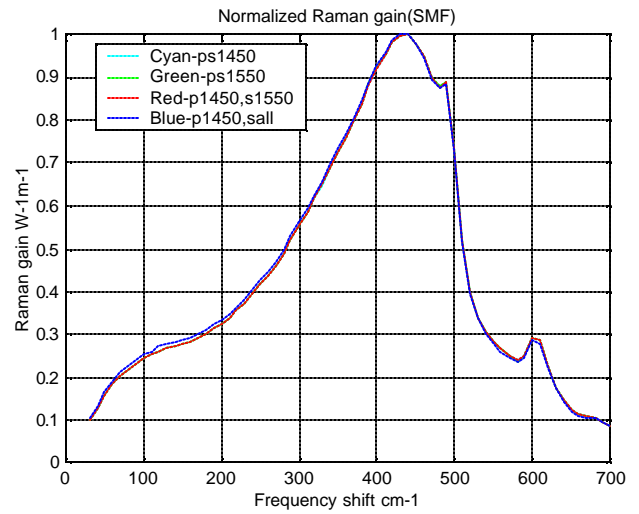


4) Z Fiber

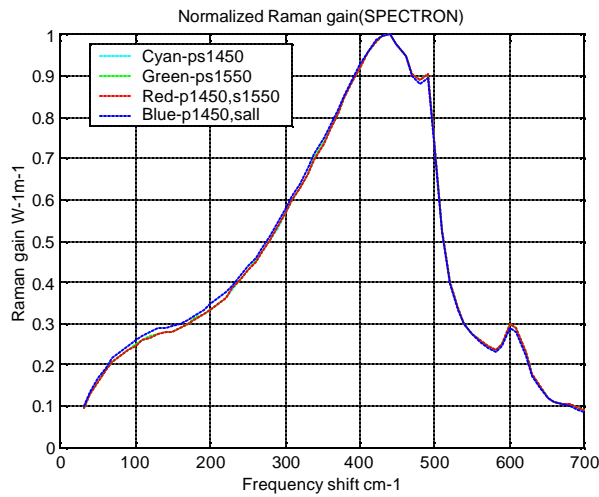
Figure 2.11 Comparison of Raman Gains of All Fiber types with Four Effective Area Approximation Schemes



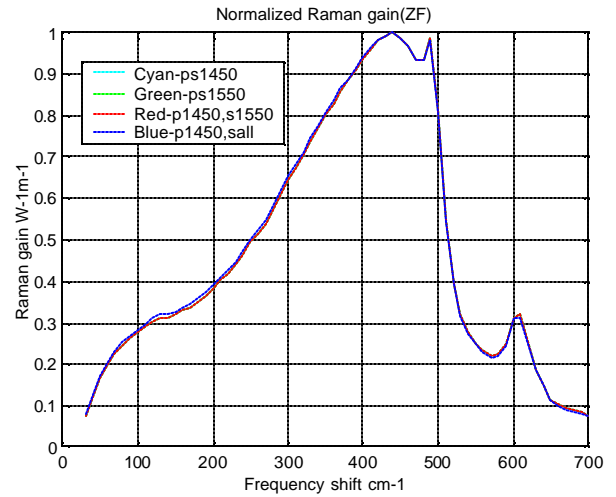
1) Dispersion Shift Fiber



2) SMF-28

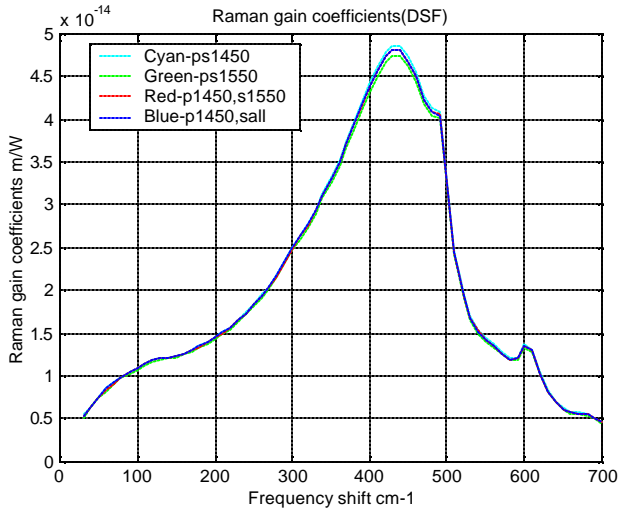


3) SPECTRAN

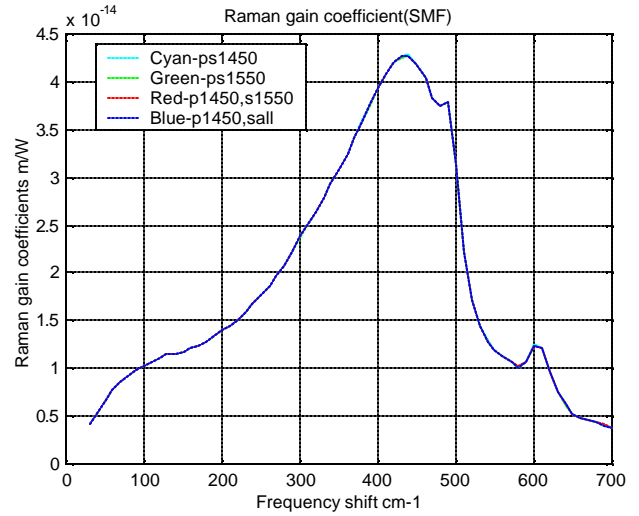


4) Z Fiber

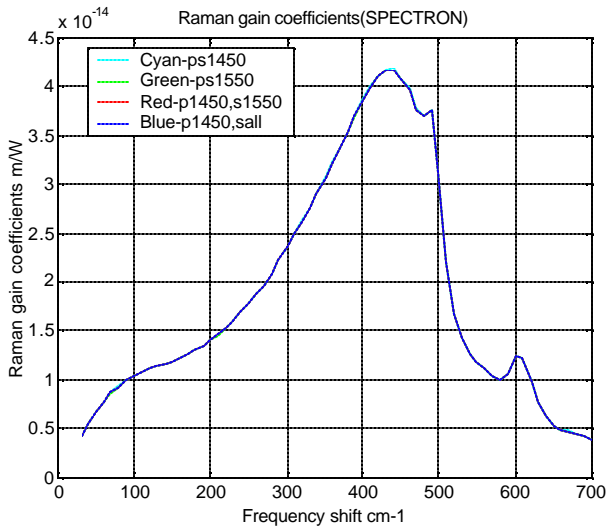
Figure 2.12 Comparison of Normalized Raman Gains of All Fiber Types with Four Effective Area Approximation Schemes



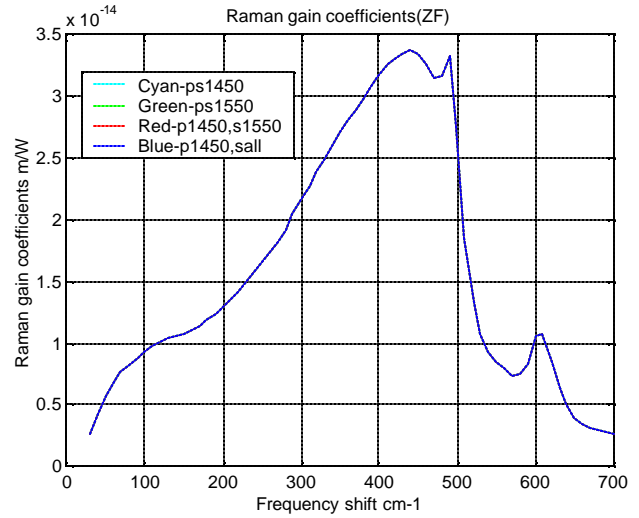
1) Dispersion Shift Fiber



2) SMF-28



3) SPECTRAN



4) Z Fiber

Figure 2.13 Comparison of Raman Gain Coefficients of All Fiber Types with Four Effective Area Approximation Schemes

2.2.3.3 A simplified calculation model for standard step index fibers

This section illustrates an approach to develop a simplified but sufficiently accurate calculation model to predict the effective Raman gain without having to calculate the $g_R(x_{GeO_2}, \mathbf{n}, r)$. As discussed in the previous section, the Raman gain profiles of STF, DSF and PSCF are close to each other. Especially for the two STF fibers, SMF and SPECTRON have almost the same Raman gain shape. This implies that it is possible to find a universal standard gain curve applicable to all fibers. The effective Raman gain of a specific fiber can be found through multiplying this standard gain curve with a constant factor, which basically is an estimated ratio of the peak gain of the under investigated fiber over that of the standard fiber.

In this section, a simplified calculation model to estimate the effective Raman gains of Standard step index fibers is proposed. The result is compared with the one obtained with the previously presented calculation model. As found in 2.2.3.1, peak gain and GeO₂ concentration of SPECTRAN fiber are both 12% less than that of the SMF-28 at 440cm⁻¹, the peak gain appears to be in linear relationship with the GeO₂ concentration, which is in fact true because the GeO₂ concentration is constant over the fiber core, and the overlapped mode fields term $\psi_p^2 \psi_s^2$ in cladding, as shown in equation 2.4, is so small that the GeO₂ concentration can be treated as a constant over the whole fiber. As a result, the $g_{TOT}(x_{GeO_2}, \mathbf{n}, r)$ from Equation 2.13 substituted into the overlap integral of Equation 2.4, can be taken out from the integral. As shown in the Equation 2.15, 2.16 and 2.17, the effective Raman gain increases linearly with GeO₂ concentration.

$$\frac{g_R}{A_{eff}} = \frac{g_{TOT}(x_{GeO_2}, \nu, r)}{A_{eff}} = \frac{n_2^2}{2n_1^2 A_{eff}} \left[\frac{A}{I_s} + \frac{B}{I_{sPeak}} \right] \quad (2.15)$$

$$A = g_{R\parallel}(SiO_2, \nu) + g_{R\perp}(SiO_2, \nu) \quad (2.16)$$

$$B = [C_{\parallel}(\nu) + C_{\perp}(\nu)] \cdot x_{GeO_2} \cdot g_{Rp\parallel}(SiO_2, \nu) \cdot \frac{I_s^3}{I_{sPeak}^3} \quad (2.17)$$

In this calculation, only peak gain needs to be considered. Thus, by substituting A with peak total gain coefficient of 1.046×10^{-13} m/W, I_s with I_{sPeak} and

$C_{\parallel}(\nu) + C_{\perp}(\nu)$ with the value at the peak gain wavelength, which is 0.0833, the above equations become

$$\frac{g_{Rpeak}}{A_{eff}} = \frac{n_2^2}{2n_1^2 A_{eff}} \left[\frac{1.046}{I_{sPeak}} + \frac{0.0833 \times 1 \times x_{GeO_2}}{I_{sPeak}} \right] \times 10^{-13} \quad (2.18)$$

I_{sPeak} value is in a unit of micron. In the case of small index difference, $\frac{n_2^2}{n_1^2}$ can be approximated to 1. Then Equation 2.18 becomes

$$g_{effpeak} = \frac{g_{Rpeak}}{A_{eff}} = \frac{1}{A_{eff} I_{sPeak}} [0.523 + 0.04165 x_{GeO_2}] \times 10^{-13} \quad (2.19)$$

The effective area at the peak gain point can be easily obtained with the mode fields at the pump wavelength and peak gain Stokes wavelength.

Through the above linear relationship between the Raman gain and GeO₂ concentration, the ratio of the peak effective Raman gain g_{eff1} of the test fiber over that of the

standard fiber g_{eff0} , $\frac{g_{eff1}}{g_{eff0}}$ can be easily achieved given a standard Raman gain curve

with its GeO₂ concentration x_{0GeO_2} , the effective peak Raman gain g_{eff0} , the

effective area A_{eff0} in μm^2 as well as the GeO₂ concentration x_{1GeO_2} , the effective

area A_{eff1} of the test fiber.

$$\frac{g_{eff1}}{g_{eff0}} = \frac{A_{eff0}}{A_{eff1}} + \frac{0.004165 (x_{1GeO_2} - x_{0GeO_2})}{I_{sPeak} \cdot A_{eff1}} \quad (2.20)$$

Finally the Raman gain curve of the test fiber can be obtained by multiplying the given standard curve with the above-calculated ratio.

In this section, the SMF-28 and SPECTRAN fibers are used to verify this model. The Raman gain curve of SMF-28 is set as the standard gain curve to estimate the Raman gain spectrum of the SPECTRAN fiber. Based on the model described above, the ratio of SPECTRAN peak gain over SMF peak gain SMF-28's peak gain value is first calculated, and then multiplied with the SMF Raman gain curve to get the estimated gain curve of SPECTRAN fiber. As shown in Figure 2.14, the resulting curve matches very well with the original one obtained through the non-simplified model. The parameters needed in the model such as GeO_2 concentrations, peak gain effective areas of SPECTRAN and SMF-28 can be found in Table 2.3.

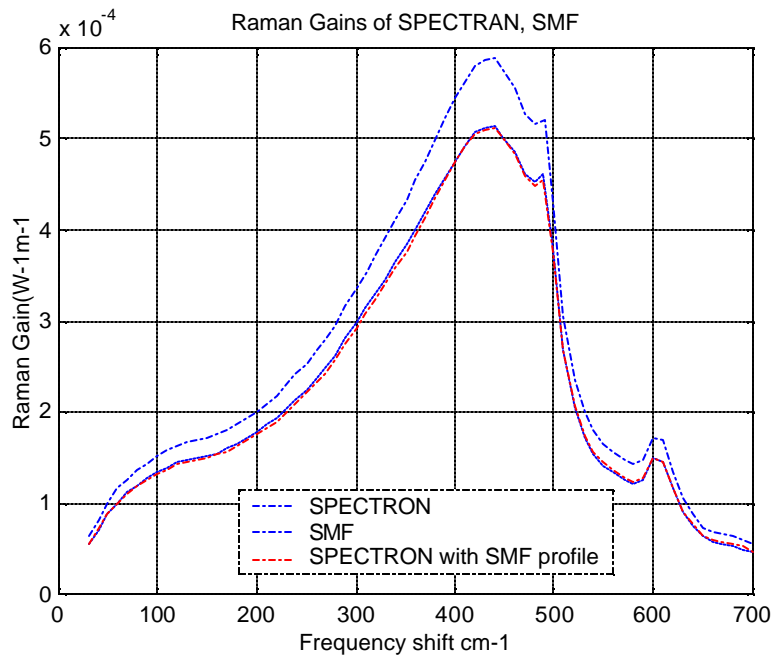


Figure 2.14 Comparison of Raman gain curves with the simplified and original calculation model

2.2.3.3 Comparison of Calculated Results From the Published Data

The calculated Raman gains for different fiber types were compared with the measured Raman gain data from several published sources [7][19-21][23][33]. Table 2.4 shows the measured effective Raman gain values (g/A_{eff}) along with the effective area (where available). Here g_1 represents the Raman gain at 150 cm^{-1} frequency shifts and g_2 represents Raman gain at peak ($430 \text{ cm}^{-1}/440 \text{ cm}^{-1}$ frequency shift). The ratio g_1/g_2 is calculated to give a measure of the deviation of the effective Raman gain curve from the standard gain curve for pure silica core fiber. In the comparison, the gain was examined at the maximum and one point well off the maximum at a frequency shift of 150 cm^{-1} .

The data were loosely grouped into three typical fiber categories for comparisons, such as pure silica core fiber, standard step index fiber and dispersion-shifted fibers. Considerable variation occurs within the categories. For example, the dispersion shifted fibers can be divided into four types, including Dispersion Shift Fiber (DSF), Non-Zero Dispersion Shift Fiber (NZ-DSF), Non-Zero Positive Dispersion Shift Fiber (NZ-DSF+), and Non-Zero Negative Dispersion Shift Fiber (NZ-DSF-). Each may provide different Raman gain values. Similar fibers from different manufacturers have different Raman gains. The effective Raman gain is seen to vary within a relatively large range, for the same category of fibers. For example, the DSF Raman gain ranges from $4.63 \times 10^{-4} \text{ W}^{-1} \text{ m}^{-1}$ to $8.4 \times 10^{-4} \text{ W}^{-1} \text{ m}^{-1}$. Much of the variation may be due differences in measurement techniques, since these procedures have not been standardized.

Table 2.5 summaries the comparison between published measurement data and calculated values of Raman gain and g_R for different fibers. For both measured and calculation cases, the DSF has the highest Raman gain while the PSCF has the least Raman gain. Calculated Raman gain however appears to be higher than that of averaged measured ones except that for the pure silica core fiber, where measured and calculated Raman gains are very close to each other. For standard fiber and dispersion-shifted fibers there is a big difference between the calculated and published values. This difference can be attributed to the fact that the calculation is made for typical fiber types

and not for the same fibers for which measurements are made in different published sources.

Fiber	A_{eff} @ 1550nm (μm^2)	g/A_{eff} (* $10^{-4}/\text{W}$ m)	G_1 (* 10^{-14} m/w)	g/A_{eff} (* $10^{-4}/\text{W}$ m)	G_2 (* 10^{-14} m/w)	g_1/g_2
		$\Delta f=150\text{cm}^{-1}$		$\Delta f=440/430\text{cm}^{-1}$		
Gray's Data [20]	Pump @ 1486nm					
SMF		1.17		3.80		0.308
NZ-DSF		1.40		4.63		0.302
Fludger's Data [21]	Pump @ 1455nm					
Allwave	80	1.0	0.8	3.59	2.88	0.279
Corning NZ-DSF	50	2.11	0.93	7.15	3.55	0.295
NDSF	80	1.15	0.84	3.93	3.12	0.292
Truewave RS	55	1.81	0.825	5.93	3.25	0.305
Corning DSF	55	2.00	1.018	6.74	3.71	0.297
Kidorf's Data [7]	Pump @ 1452nm					
PSCF		1.33		4.28		0.311
D.Hamoir	Pump					

Pump: [19]	@1486nm					
NZDSF+	55	2.43	1.34	8.4	4.62	0.289
NZDSF-	55	2.26	1.24	7.7	4.24	0.294
TeraLight	67	1.69	1.13	5.7	3.82	0.296
SMF	83	1.30	1.08	4.5	3.74	0.289
PSCF	78	1.30	1.01	4.3	3.36	0.302
Puse Silica Stolen [23]	Stokes @1000nm		1.12		3.53	0.318
Tycom(1): [33]	Pump@ 1480nm					
Truewave (Average)	50.9			7.18	3.65	0.299
Leaf (Average)	71.4			4.95	3.53	0.299
LS (Average)	51.65			7.42	3.83	0.299
Sumitumo Z	79.4			3.51	2.79	0.299
IDFX	28.7			16.09	4.62	0.299
HFD2	53.7			6.96	3.74	0.299
LMF1	77.6			4.72	3.66	0.299
5D	71.2			3.97	2.83	0.299
Tycom(2)						
DSF						0.291

SMF						0.279
PSCF						0.309

Table 2.4 Measured Raman Gain For Different Transmission Fiber Types

It also can be seen in Table 2.5 that the PSDF has the largest g_1/g_2 , while the STF has the least; at the same time, the simulation results indicate that DSF has the least g_1/g_2 . However g_1/g_2 values for STF and DSF in both cases are close to each other. All the published data shows that the second peak of the gain curve suppresses with Ge-doping, and the gain peak moves to the low frequency shift side as the GeO_2 increases, which is in good agreement with the calculation results.

	PUBLISHED DATA			CALCULATED DATA		
Pump=1450nm	PSCF	STF	DSF	PSCF	STF	DSF
g_R	0.305	0.292	0.296	0.327	0.294	0.286
Raman Gain (*1e-4w-1m-1)						
Average	4.01	4.07	7.10	3.95	5.53	10.3
Maximum	4.32	4.52	8.43			
Minimum	3.51	3.80	4.63			

Table 2.5 Comparisons between the Calculated and Published Measurement D For Different Transmission Fiber Types

Summary

We estimated Raman gain for pure silica core fiber, standard single mode fiber and dispersion- shifted fiber. It was noticed that dispersion-shifted fiber provides the highest effective Raman gain among the fibers investigated. It was also observed that pump at

1450 nm and signal at 1550 nm can be used to approximate the absolute effective area in calculating the gain spectrum. The calculated results were compared with the measured results obtained from various published sources. The calculated results are found to be in good qualitative agreement with the measured ones. Good quantitative agreement between calculation and published measurements is obtained for the PSCF. However, the calculated effective Raman gains for the STF and DSF are higher than even the maximum published values. The discrepancies in quantitative results between the two might be attributed to the fact that the calculations are made for some typical fiber types and not for the same fibers which various published sources used for the measurements. Secondly the published sources themselves have discrepancies in gain values for the same kind of fibers. Finally, much of the variation may be due differences in measurement techniques, since these procedures have not been standardized. As a result, it is necessary to make our own measurements to verify if the calculation model is valid.

Chapter 3 - Measurement of Raman Gain in Optical Fibers

In this chapter, the experiment setup for the measurement of Raman gain of a step index fiber is given. In order to get accurate experimental results, some considerations are discussed. The measurement results are then analyzed and compared with the simulation ones.

3.1 Experimental Setup of Fiber Raman Gain Measurement

The purpose of this experiment is to measure the peak Raman gain in optical fibers and verify the data with the simulation results mentioned in the previous chapter. This experiment focuses on the effective Raman gain, also called Raman gain coefficient over effective area, $\frac{g_R}{A_{eff}}$, which is a more practical parameter than the Raman gain coefficient in a Raman amplifier. Knowing this number can give us a projection of what kind of signal gain can be achieved within a specific fiber given its length and attenuation parameters at pump and signal wavelengths. A measurement of the actual Raman gain coefficient is more complicated since the gain coefficient depends on GeO₂ concentration, which varies across the index profile. For this reason, only $\frac{g_R}{A_{eff}}$ is investigated and measured utilizing the so-called pump on and off technique. However, we may estimate the peak effective Raman gain coefficients by multiplying the measured $\frac{g_R}{A_{eff}}$ with calculated A_{eff} at pump and peak signal wavelengths or the average of measured A_{eff} s at pump and signal peak wavelengths.

Based on the equation 2. 1, the Raman gain is determined. When pump is off, the output signal power is attenuated due to the fiber loss.

$$P_{S_off}(L) = P_S(0)\exp(-\alpha_s L) \quad (3.1)$$

When pump is on, the signal is amplified and the output signal power becomes:

$$P_{S_on}(L) = P_S(0) \exp\left(\frac{g_R(v)P_0L_{eff}}{KA_{eff}} - a_s L\right) \quad (3.2)$$

G, the pump on/off gain in dB, is determined by

$$G = 10 \log_{10}\left(\frac{P_{S_on}(L)}{P_{S_off}(L)}\right) \quad (3.3)$$

By substituting equations (3.1) and (3.2), the effective Raman gain is obtained

$$\frac{g_R}{KA_{eff}} = \frac{G}{4.343 \cdot L_{eff} \cdot P_{pump}} \quad (3.4)$$

where L_{eff} is the effective length calculated by the equation (2.1), P_{pump} is the pump power launched into the fiber spool, $\frac{g_R}{KA_{eff}}$ is depolarized effective Raman gain.

The Raman gain measurement was performed on a step index single mode fiber by using the setup shown in Figure 3.1.

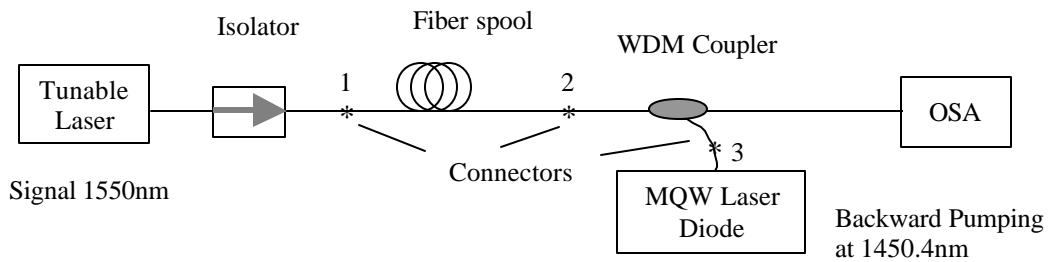


Figure 3.1 Experimental setup for measuring Raman gain

Backward pumping was used in order to cancel out polarization effects and amplitude fluctuations from pump to signal. An isolator was placed in front of the Tunable laser source to prevent the pump light from entering into this laser source. The optical spectrum analyzer (OSA) measured the output signal power in the cases of pump-on and pump-off. The major advantage in this setup is the fact that the signal input power, the losses due to fiber attenuation at the signal wavelength, imperfect fiber connectors or system function of the Wavelength Division Multiplexing (WDM) coupler and isolator need not to be known. All these factors are cancelled out by calculating the Raman on-off gain.

3.2 Experimental Results

The fiber under test is a 22.195 km long SPECTRAN fiber and has a step index profile with a pure silica cladding and GeO₂-doped silica core. The fiber was made with VAD process so there is no index dip at the center of the core. This is an important feature for accurate calculation of Raman gain of this fiber because there is no radial variation of Ge concentration across the core. This fiber is also extremely uniform along its length. The fiber core diameter is 8.3 microns and the core cladding index difference is 0.00462 as measured with a York fiber index profiler and shown in previous chapter. The cutoff wavelength and MFD at 1310 nm of this fiber sample were calculated using the above measured fiber parameters, which are consistent with the manufacturer's value for the cutoff wavelength of 1.216 microns and MFD of 9.2 microns at 1310nm.

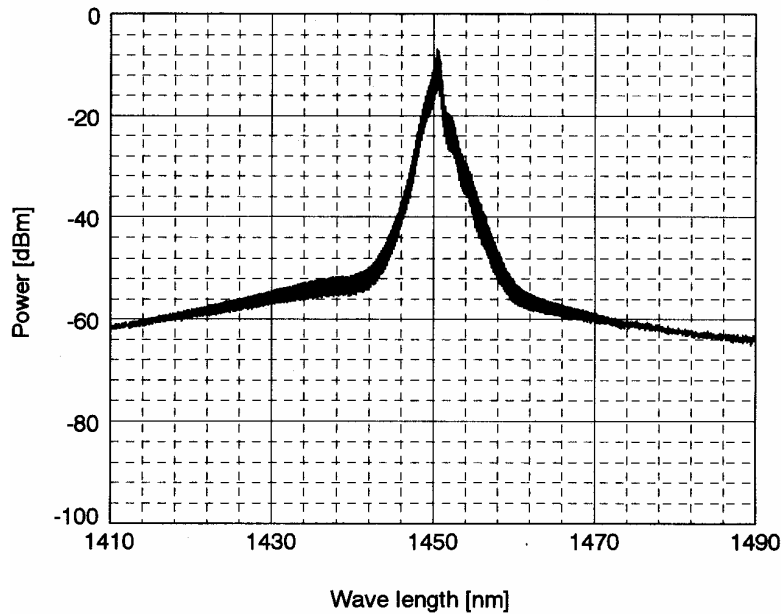


Figure 3.2 Spectrum of the pump source

The pump source used was a Multi-Quantum Well (MQW) laser diode with Fiber Bragg Grating (FBG) centered at a wavelength of 1450.4 nm, its spectrum is shown in Figure 3.2. The 3dB bandwidth is around 0.8nm (0.114THz). As discussed in the previous chapter, the pump bandwidth is required to be much less than the bandwidth of the gain curve, while much larger than the 100 MHz (Spontaneous Brillouin scattering bandwidth) to prevent stimulated Brillouin scattering occurring in the fiber. SBS would largely deplete the pump power and cause measurement error. Pump power measured at one of WDM coupler ends, connector number 2, shown in figure 3.1, was 116.48 mW and then corrected for the reflection loss, which gives pump power equal to 120.39 mW. The reflection loss caused by the end face of the fiber is about 3.25% of the pump power.

The signal source was a tunable laser set at 1550 nm (peak Raman gain wavelength). It is not necessary to know the exact signal power because of the pump on/off method, however, based on assumption that the amplification of Stokes does not significantly deplete the pump, the signal power should be much less than the pump power. The signal power measured from the laser source connector is 50uW.

The measured loss of the fiber at the pump wavelength using cut back method with a white light source was 0.261 dB/km giving an effective length of 12.249 km.

Figure 3.3 shows the spectra of the pump on/off output signals.

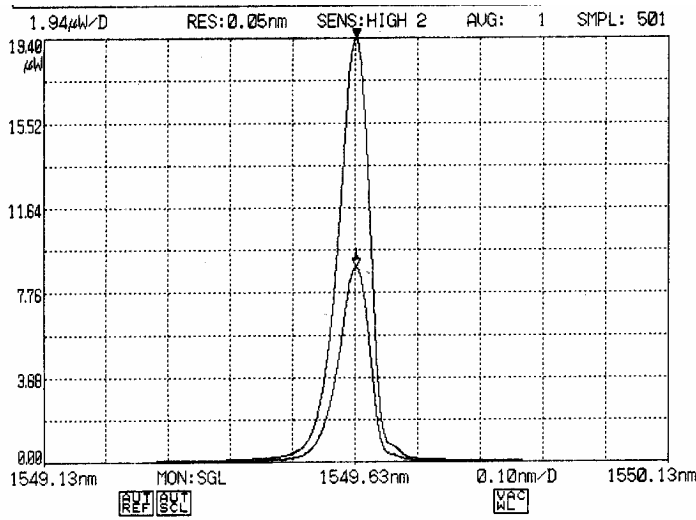


Figure 3.3 Pump on/off Optical Gain in dB

Taking integrals of the spectra of the pump on/off output signals and dividing the resulting signal pump-on power with the pump-off power gives us the measured pump on/off signal gain, which was 3.324 in dB. Substituting the measured pump power and effective length values into equation (3.4), g/A_{eff} was calculated to be $5.19 \times 10^{-4} \text{ m}^{-1} \text{ W}^{-1}$, while the simulation result is $5.175 \times 10^{-4} \text{ m}^{-1} \text{ W}^{-1}$ as shown in Table 2.3. The 0.29% difference between the simulation result and the measurement data shows an excellent agreement.

In conclusion, the calculation model of relating the spontaneous Raman cross-sections to the stimulated effective Raman gains and gain coefficients are validated by the measurement result.

Chapter 4 – Conclusions

4.1 Conclusions

In this thesis, a calculation model was developed to predict the Raman gains and Raman gain coefficients achieved in different GeO₂-doped silica fibers given their fiber profiles. The following goals have been met:

- 1) Study of some major factors affecting the Raman gain in a fiber: the theoretical background for relating the spontaneous Raman cross-section to the effective Raman gains and gain coefficients of different GeO₂-doped fibers was studied. The effect of the mode field penetrating into the fiber cladding was included in the calculation model.
- 2) Comparison of the simulation data with the published measurement data: The calculated results were compared with the measured results from various published sources. The calculated results are found to be in good qualitative agreement with the measured ones.
- 3) Development of the simplified but sufficiently accurate calculation model: To simplify the calculations, an optimized effective area approximation scheme was obtained by taking approximated signal wavelengths. Also a simplified calculation model to estimate the effective Raman gains of Standard step index fibers without having to calculate the $g_R(x_{GeO_2}, \mathbf{n}, r)$ is proposed and verified.
- 4) Verification of the calculation model by conducting our own measurements: The measurement of the peak Raman gain using pump on/off method is performed upon a step index GeO₂-doped silica fiber, which is in excellent agreement with the calculated result and thus supports this Raman gain calculation model.

In conclusion, this calculation model is accurate to get the effective Raman gains in a GeO₂-doped fiber given its fiber profile, it can give us a projection of how much signal gain can be achieved in a specific fiber given its length and attenuation parameters at

pump and signal wavelengths. Moreover, this model is of help in understanding the material and fiber structure dependence of Raman amplification.

4.2 Future Work

This simulation model calculates the small signal Raman gain as a function of GeO₂ concentration in optical fibers. From this work, several investigations can be conducted.

The current model investigates the Raman amplification in a fiber when pumping at a single wavelength. In fact, recent progress in the Raman amplification area is the application of the multi-wavelength pumped Raman amplifier. This technology can provide broader and flatter gain spectrum, which is of significance to the wavelength division multiplexed system. The current model can be modified for the estimation of the net Raman gain for multi-wavelength pumped Raman amplifier. This is related to the superposition of the Raman gain spectra from individual pumps. Moreover, efforts of adjusting the pump wavelengths to flatten and broaden the gain bandwidth are needed.

Another improvement would be to develop a more simplified but sufficiently accurate calculation model to predict the effective Raman gain in any fiber type without having to calculate the $g_R(x_{GeO_2}, \mathbf{n}, r)$. As discussed in the chapter 2, the shapes of the effective Raman gains of GeO₂-doped fibers are similar. This may lead us to a possible solution of finding the effective Raman gain of a fiber through multiplying a standard gain curve with a constant factor corresponding to the fiber type, in which the constant factor depends on the GeO₂ concentration.

References

1. Yasuhiro Aoki, "Fiber Raman amplifier properties for applications to long-distance optical communications", *Optical and Quantum Electronics*, Vol.21, spec. Issue, pp. S89-S104, 1989
2. P.B. Hansen, L.Eskildsen, S.G. Grubb, A.J. Stentz, T.A. Strasser, J.Judkins, J.J. DeMarco, R. Pedrazzani, and D.J. DiGiovanni, "Capacity Upgrades of Transmission Systems by Raman Amplification", *IEEE Photonics Technology Letters*, Vol. 9, No.2, pp. 262-264, Feb., 1997.
3. L.F. Mollenauer, R.H. Stolen, and M.N. Islam, "Experimental demonstration of Soliton propagation in long fibers: loss compensated by Raman gain", *Optics Letters*, Vol.10, No. 5, pp. 229-231, 1985
4. T.N. Nielsen, "Raman Amplifier in WDM systems", *1999 IEEE LEOS Annual Meeting Conference Proceedings*, Vol.2, pp.471-472, NJ, USA, 1999
5. H. Suzuki, J. Kani, H. Masuda, N. Takachio, K. Iwatsuki, Y. Tada, and M. Sumida, "25 GHz-spaced, 1 Tb/s (100*10 Gb/s) super dense-WDM transmission in the C-band over a dispersion-shifted fibre cable employing distributed Raman amplification", *25th European Conference on Optical Communication. ECOC '99 Conference*, pp.30-31, Paris, France. 1999
6. P.B. Hansen, et al., "Rayleigh scattering limitations in distributed Raman pre-amplifiers", *IEEE Photonics Technology Letters*, Vol.10, No.1, pp.159-161, 1998
7. Howard Kidorf, Karsten Prottwitt, Morten Nissov, Matthew Ma, and Eric Rabarijana, "Pump Interactions in 100-nm Bandwidth Raman Amplifier," *IEEE Photonics Technology Letters*, Vol.11, No.5, pp. 530-532, May 1999
8. Victor E. Perlin, Herbert G. Winful, "On distributed Raman amplification for Ultrabroad-band Long-Haul WDM systems", *Journal of Lightwave Technology*, Vol. 20, No. 3, pp.409-416, March 2002
9. Data sheet from Amonics, www.amonics.com.
10. R.H. Stolen, E.P. Ippen, and A.R. Tynes, "Raman oscillation in glass optical waveguide", *Applied Physics Letters*, Vol.20, No.2, pp.62-64, 1972

11. C. Lin and R.H. Stolen, "Backward Raman amplification and pulse steepening in silica fibres", *Applied Physics Letters*, Vol.29, No.7, pp.428-431. 1976
12. F.L. Galeender, J.C. Mikkelsen, R.H. Geils, and W.J. Mosby, "The relative Raman cross sections of vitreous SiO₂, GeO₂, B₂O₃ and P₂O₅", *Applied Phys. Letters*, Vol. 32, No.1, pp.34-36, 1978,
13. E.P. Ippen, C.K.N. Patel, and R.H. Stolen, "Broadband tunable Raman –effect devices in optical fibers", *U.S. Pat.* 3,705,992, 1971
14. J.Hegarty, N.A.Olsson, and L.Goldner, "CW pumped Raman preamplifier in a 45 km-long fibre transmission system operating at 1.15um and 1Gbit/s", *Electronics Letters*, Vol.21, No.7, pp.290-292, 1985
15. T. Horiguchi, T. Sato, and Y. Koyamada, "Stimulated Raman amplification of 1.6um-band pulsed light in optical fibers", *IEEE Photonics Technology Letters*, Vol.4, No.1, pp.64-66, 1992.
16. E.M. Dianov, "Raman fiber amplifiers for the spectral region near 1.3um", *Laser Physics*, Vol.6, No.3, pp.579-580, 1996.
17. T.N. Nielsen, et al., "3.28Tb/s (82*40Gb/s) transmission over 3*100km nonzero-dispersion fiber using dual C- and L-band hybrid Raman/erbium doped inline amplifiers", *Optical Fiber Communications, Technical Digest Postconference Edition. Trends in Optics and Photonics*, Vol.37, Opt. Soc. America. Part vol.4, pp.236-238, 2000.
18. Y. Emori, K. Tanaka, and S. Namiki, "100 nm bandwidth flat-gain Raman amplifiers pumped and gain-equalised by 12-wavelength-channel WDM laser diode unit", *Electronics Letters*, Vol.35, No.16, pp.1355-6, 1999.
19. D. Hamoir, N. Torabi, A. Bergonzo, S. Borne and D. Bayart, "Raman spectra of line fibers measured over 30THz, " *Tech Digest, Symposium on Optical Fiber measurements*, pp.147-150, 2000
20. S. Gray, "Raman Gain Measurements in optical fibers," *Technical Digest, Symposium on Optical Fiber Measurements*, pp.151-156, 2000,
21. C. Fludger, A. Maroney, N. Jolley, R. Mears, "An analysis of the improvements in OSNR from distributed Raman amplifiers using modern transmission fibers, " *Optical Fiber Communication Conference. Technical Digest Postconference*

- Edition. Trends in Optics and Photonics*, Vol.37. Opt. Soc. America., Part vol.4, pp.100-102, DC, USA, 2000.
22. F.L. Galeener and G. Lucovsky, "Longitudinal optical vibrations in glasses: GeO_2 and SiO_2 ", *Physical Review Letters*, Vol.37, No. 22, pp.1474-1478, 1976
 23. R.H. Stolen, C. Lee, and R.K. Jain, "Development of the stimulated Raman spectrum in single-mode fibers," *Journal of Optical Society of America B*, Vol.1, No.4, pp.652-657, 1984
 24. R.H. Stolen, "Polarization effects in fiber Raman and Brillouin lasers", *IEEE Journal of Quantum Electronics*, QE-15, pp.1157, 1979
 25. R. H. Stolen, Stewart E. Miller, and A. G. Chynoweth, Nonlinear properties of Optical Fibers, *Optical Fiber Telecommunications*. New York: Academic, Ch.5, pp.125-150, 1979
 26. N. Shibata, M. Horigudhi, and T. Edahiro, "Raman spectra of binary high-silica glasses and fibers containing GeO_2 , P_2O_5 and B_2O_3 ", *Journal of Non-Crystalline Solids*, Vol.45, pp.115-126, 1981
 27. S.T. Davey, D.L. Williams, B.J. Ainslie, W.J.M. Rothwell and B.Wakefield, "Optical gain spectrum of GeO_2 - SiO_2 raman fibre amplifiers", *IEE Proceedings*. Vol. 136, Pt. J. No. 6, December 1989.
 28. R.H. Stolen, "Issues in Raman Gain measurements", *Technical Digest Symposium on optical Fiber Measurements*, pp.139-142, 2000,
 29. R.H. Stolen, "Raman scattering and infrared absorption from low lying modes in vitreous SiO_2 , GeO_2 and B_2O_3 ", *Physics and Chemistry of Glasses*, Vol.11, No.3, pp.83-87, 1970
 30. W.A. Reed, Private communications, 1996
 31. R.H. Stolen, William A. Reed, K.S. Kim and G.T. Harvey, "Measurement of the nonlinear refractive index of long dispersion-shifted fibers by self-phase modulation at 1.55 μm ", *Journal of Lightwave Technology*, Vol.16, No.6, June 1998.
 32. T. Izawa and S. Sudo, *Optical Fibers: Materials and Fabrication*. D. Reidel Publishing Company.
 33. V.J. Mazurczyk, "Measurement of the Spectral dependence of the Raman gain coefficient for different fiber types", (DocOpen#58337, unpublished), Tycom.

Vita

Yuhong Kang was born in Hunan Province, P. R. China. After graduating from Huazhong University of Science and Technology with a Bachelor of Science degree in Optics Engineering in 1991, she attended Guangdong Nortel Telecommunications Equipment Ltd. In 1996, she then worked at Xi'an Institute of Optics and Precision Mechanics, Academia Sinica as an Optoelectronics Engineer. In 2001, she joined Fiber and Electro-optics Research Center at Virginia Tech as a Graduate Research Assistant. She earned her Master of Science degree in Electrical Engineering from Virginia Tech in December 2002.